Atmos. Chem. Phys. Discuss., 9, 2319–2380, 2009
www.atmos-chem-phys-discuss.net/9/2319/2009/

Atmospheric Chemistry and Physics Discussions

This discussion paper is/has been under review for the journal *Atmospheric Chemistry and Physics (ACP)*. Please refer to the corresponding final paper in *ACP* if available.

The impact of MM5 and WRF meteorology over complex terrain on CHIMERE model calculations

A. de Meij[1], A. Gzella[1], P. Thunis[1], C. Cuvelier[1], B. Bessagnet[2], J. F. Vinuesa[1], and L. Menut[3]

[1]European Commission – DG Joint Research Centre, Institute for Environment and Sustainability, 21020 Ispra, Italy
[2]INERIS, Institut National de l'Environnement industriel et des Risques, Parc Technologique ALATA, 60550 Verneuil-en-Halatte, France
[3]Laboratoire de Météorologie Dynamique, Institut Pierre-Simon Laplace, Ecole Polytechnique, Palaiseau, France

Received: 17 November 2008 – Accepted: 13 December 2008 – Published: 26 January 2009

Correspondence to: A. de Meij (alexander.de-meij@jrc.it)

Published by Copernicus Publications on behalf of the European Geosciences Union.

Abstract

The objective of this study is to evaluate the impact of meteorological input data on calculated gas and aerosol concentrations. We use two different meteorological models (MM5 and WRF) together with the chemistry transport model CHIMERE. We focus on the Po valley area (Italy) for January and June 2005.

Firstly we evaluate the meteorological parameters with observations. The analysis shows that the performance of both models is similar, however some small differences are still noticeable.

Secondly, we analyze the impact of using MM5 and WRF on calculated PM_{10} and O_3 concentrations. In general CHIMERE/MM5 and CHIMERE/WRF underestimate the PM_{10} concentrations for January. The difference in PM_{10} concentrations for January between CHIMERE/MM5 and CHIMERE/WRF is around a factor 1.6 (PM_{10} higher for CHIMERE/MM5). This difference and the larger underestimation in PM_{10} concentrations by CHIMERE/WRF are related to the differences in heat fluxes and the resulting PBL heights calculated by WRF. In general the PBL height by WRF meteorology is a factor 2.8 higher at noon in January than calculated by MM5. This study showed that the difference in microphysics scheme has an impact on the profile of cloud liquid water (CLW) calculated by the meteorological driver and therefore on the production of SO_4 aerosol.

A sensitivity analysis shows that changing the Noah Land Surface Model (LSM) for the 5-layer soil temperature model, the calculated monthly mean PM_{10} concentrations increase by 30%, due to the change in the heat fluxes and the resulting PBL heights.

For June, PM_{10} calculated concentrations by CHIMERE/MM5 and CHIMERE/WRF are similar and agree with the observations. Calculated O_3 values for June are in general overestimated by a factor 1.3 by CHIMERE/MM5 and CHIMRE/WRF. The reason for this is that daytime NO_2 concentrations are a higher than the observations and nighttime NO concentrations (titration effect) are underestimated.

ACPD

9, 2319–2380, 2009

1 Introduction

Aerosols play an important role in health effects (respiratory and cardiovascular disease, Moshammer and Neuberger, 2003), pollution, eutrophication/acidification of aquatic and terrestrial ecosystems and radiative forcing (absorbing and scattering of solar radiation, Kaufman et al., 2002). Ground-based measurement networks provide information about the atmospheric conditions at a particular time and location and can not be used alone for policymaking to establish effective strategies for air emissions reduction policy. The atmospheric chemistry-transport-dispersion models (CTMs) have the advantage that they can be used to complement monitoring data, assess the effects of future changes in aerosol and aerosol precursor emissions and to study the impact of source pollutants on air quality elsewhere.

Each atmospheric chemistry transport model includes a specific sequence of operations, with specific input data, such as emissions and meteorology to calculate gas and aerosol concentrations.

Uncertainties in the estimation of gases and primary aerosols in the emission inventories (De Meij et al., 2006), aerosol dynamics (physical transformations, dry and wet removal, transport), meteorological factors (temperature, humidity, wind speed and direction, precipitation, cloud chemistry, vertical mixing), the impact of orography on meteorological parameters (Carvalho et al., 2006), the impact of horizontal resolution of meteorology on model calculations (Menut et al., 2005) all contribute to uncertainties in the calculated gas and aerosol concentrations.

The formation of aerosols are known to be nonlinearly dependent on meteorological parameters such as temperature, humidity and vertical mixing (Haywood and Ramaswamy, 1998; Penner et al., 1998) and the concentrations of precursor gases (West et al., 1998). Clouds (chemical transformation), precipitation (wet removal of the aerosols) and the changes in the wind profiles or turbulence fields (topography and land use induced) determine how the pollutants are dispersed and transported over distance. A good estimate of meteorological variables in the meteorological datasets

ACPD
9, 2319–2380, 2009

is therefore crucial for calculating gas and aerosol impacts on air quality and climate change, and evaluating coherent reduction strategies.

The main objective of this study is to evaluate the impact of meteorological input data on calculated aerosol concentrations. We study the central Po valley (northern Italy), which is one of the most polluted, industrialized and densely populated areas in Europe. We focused our analysis on the year 2005 and particularly on a winter month (January 2005) and a summer month (June 2005), to highlight the impact of different meteorological conditions prevailing in winter and summer on the calculated gas and aerosol concentrations. To this end we performed simulations with the CHIMERE model (http://www.lmd.polytechnique.fr/CHIMERE/), using two different meteorological models, the Mesoscale Meteorological model (MM5, Grell et al., 1994) and the Weather Research and Forecasting model (WRF, http://wrf-model.org/index.php). So far, work has been done in comparing MM5 and WRF simulated meteorological parameters with observations (Zhong et al., 2007; Michelson and Bao, 2006), and the impact of MM5 and WRF on ozone calculated values (Soong et al., 2006). To our knowledge, no studies have been performed in evaluating the impact of MM5 and WRF on calculated aerosol species.

Section 2 deals with the description of the simulations, the air chemistry transport model, the meteorological models and the emission inventory. In Sect. 3 a description of the measurement data is given. In Sect. 4 the results are presented. We discuss the results in Sect. 5 and we finish with conclusions in Sect. 6.

2 Methodology

The CHIMERE model (Bessagnet et al., 2004) is used to simulate air quality over the Po valley area for January and June 2005 based on the meteorological data sets provided by MM5 and WRF. More details regarding the atmospheric chemistry and meteorological models are given in Sect. 2.1 and 2.2, respectively.

We start our study by evaluating the meteorological parameters such as temperature,

relative humidity, wind direction and wind speed, calculated by both weather prediction models. The modelling results were compared with meteorological observations for the year 2005, given by the monitoring network of the Regional Agencies for Environment Protection in Lombardy (Agenzia Regionale per la Protezione dell' Ambiente, ARPA Lombardia, www.arpalombardia.it).

Then we evaluate the calculated aerosol (PM_{10}) and ozone (O_3) concentrations, using the CHIMERE model with MM5 and WRF results as input data, by comparing the model calculated concentrations with measurements from the EMEP station and measurements from the ARPA networks (Lombardy and Veneto). We focus on PM_{10} and O_3 because these pollutants are prevailing the most in the Po valley and are commonly measured at most of the air quality monitoring stations. More details regarding the measurement networks are given in Sect. 3.

Four simulations are performed with CHIMERE, two simulations with MM5 meteorology (CHIMERE/MM5) for January 2005 and June 2005, and two simulations with WRF meteorology (CHIMERE/WRF) for January and June 2005. For the four simulations, a spin-up time of 4 days is applied in order to initialize the model.

2.1 Description CHIMERE model

CHIMERE is an off-line chemistry transport model, driven by a meteorological driver, such as MM5 (Grell et al., 1994) or WRF (http://wrf-model.org/index.php).

The complete chemical mechanism in CHIMERE is called MELCHIOR1 (Lattuati, 1997, adapted from the original EMEP mechanism, Hov et al., 1985), which describes more than 300 reactions of 80 species. The reduced mechanism MELCHIOR2 includes 44 species and about 120 reactions, derived from MELCHIOR1 (Derognat et al., 2003).

Processes like chemistry, transport, vertical diffusion, photochemistry, dry deposition, in-cloud and below cloud scavenging and SO_2 oxidation in clouds are included in the model. Transport is computed with the Piecewise Parabolic Method (PPM) developed by Colella and Woodward (1984). Vertical diffusion is parameterized using a diffusivity profile (Troen and Mahrt, 1986) depending on boundary layer height, rough-

ness velocity and convective velocity scale. Photolysis rate constants needed for the photochemical reactions are calculated using the TUV Tropospheric Ultra-violet visible) module (Madronich and Flocke, 1998) and depend on altitude. Dry deposition is calculated with the resistance analogy (Wesely, 1989) and is the inverse value of three resistances in series: the aerodynamic resistance, the resistance in the viscous sublayer between the surface and the turbulent boundary layer, and the surface resistance. Deposition velocities are calculated per species and land surface type.

In cloud and below cloud scavenging processes are included in the model. Cloud chemistry is an important source for sulphate in the atmosphere, which involves the oxidation of SO_2 by H_2O_2 and O_3 in clouds. The formation of secondary organic aerosol is included in the model. More details regarding the parameterizations of the above mentioned processes are described in Bessagnet et al., 2004 and references therein.

The thermodynamic equilibrium model ISORROPIA (Nenes et al., 1998) is used to calculate the equilibrium partitioning of the gas-liquid-solid aerosol phase of various aerosols compounds (e.g. $SO_4^=$, NO_3^-, NH_4^+, Na^+, Cl^-).

CHIMERE has 8 size bins for the aerosols. The first six size bins are in the $PM_{2.5}$ range (0.0–40 nm, nucleation mode; 40 nm–0.15 μm Aitken/accumulation; 0.15 μm–0.62 μm, accumulation; 0.62 μm–2.5 μm accumulation/coarse mode; 2.5 μm–10 μm coarse mode and from 10 μm–40 μm, super coarse mode). Within each size bin the aerosols are assumed to be mono-disperse and have identical chemical composition. The aerosols calculated by CHIMERE are PPM (organic carbon, black carbon and anthropogenic dust), sulphates, nitrates, ammonium, secondary organic aerosols (anthropogenic and biogenic organic aerosol, Pankow et al., 1994, 2001) and aerosol water. The aerosols are assumed to be internally mixed.

In CHIMERE, aerosol dynamics include nucleation, coagulation, condensation and evaporation. Nucleation is an important process for new particle production. The nucleation parameterization is based on Kulmula et al., 1998, using sulphuric acid vapour concentrations. The aerosol size distribution changes due to coagulation, reducing the number of particles and a change of the aerosol mass in each size bin. These pro-

ACPD
9, 2319–2380, 2009

cesses are particularly efficient for the smaller particles in the nucleation and Aitken modes. Particle collision (coagulation) is a result of the Brownian diffusion. The Brownian diffusion coefficients are based on Fuchs (1964). The "new" sized aerosols are moved in the correct size bin at each time iteration. Condensation and evaporation of vapours is one of the processes responsible for the growth, the decrease of the number of atmospheric particles (especially for the nucleation and Aitken mode), and for changing the aerosol chemical composition. The condensation and evaporation processes are driven by the difference between ambient gas concentration and the concentration at the particle surface. In Table 1 an overview is given of the chemical and physical processes which are included in CHIMERE. A more detailed description of the processes in CHIMERE is described in Bessagnet et al. (2004).

The lateral boundary conditions of gas species are monthly average values and are taken from the INCA model (http://www-lsceinca.cea.fr/welcome_real_time.html). The boundaries conditions of aerosols are taken from the monthly mean aerosol concentrations provided by the larger scale model GOCART (Ginoux et al., 2001, 2004). CHIMERE consists of 8 hybrid sigma pressure levels, up to 500 hPa (±5500 m). The domain (approximately 300×300 km, centred at 45.0° N, 10.0° E) covers most of the Po Valley, Italy, including southern part of the Alps, see Fig. 1.

2.2 Description meteorological input

To calculate gas and aerosol concentrations, CHIMERE needs meteorological parameters such as humidity, air temperature, pressure, wind fields and planetary boundary layer height. The meteorological input for the air chemistry model is taken from numerical weather prediction model. For this study we used two different meteorological models, MM5 and WRF. Both developed at National Center for Atmospheric Research (NCAR). In the Sect. 2.2.1 and 2.2.2, we describe the two meteorological models.

The meteorological data sets used for the study were created within the Po valley air quality Model Inter-comparison (POMI) exercise, which is coordinated by the Institute of Environment and Sustainability, JRC, Ispra, Italy (http://aqm.jrc.it/POMI/). The POMI

exercise is focused on the area of the Northern Italy and two nested domains are set up there for meteorological data. WRF operates on the 5 km and 2.5 km resolution domains (one-way nested) and MM5 – on the 6 km and 2 km resolution domains (two-way nested).

It should be noticed that the choice of the parameterization in MM5 and WRF is not always the same. The choice of the model setup in MM5 and WRF is based on previous studies and recommendations by NCAR.

Both MM5 and WRF use meteorological initial conditions and lateral boundary conditions from 6 h analyses from the NCEP Global Final (FNL) Analyses. Data produced during pre-processing and modelling simulations of MM5 and WRF are in the Lambert conformal projection.

2.2.1 Description of MM5

The PSU/NCAR mesoscale model MM5 (3.7.4) is a limited-area, non-hydrostatic or hydrostatic, terrain following sigma-coordinate model designed to simulate or predict mesoscale and regional scale atmospheric circulations (Grell et al., 1994).

The initial resolution used for implementing terrain data in the proposed study is based on the 30 s database (~0.9 km spatial resolution). Land use, vegetation, land-water mask, soil types, vegetation fraction and deep soil temperature are provided for this resolution. 25 categories of vegetation/land use and land-water mask data for global coverage are available. Vertical discretization involves 20 levels up to 8 km.

The model is set using the Simple ice scheme for microphysics (Dudhia, 1989), the planetary boundary layer (PBL) Medium Range Forecast Model (MRF) scheme (Hong and Pan, 1996) and the Noah land surface model (Chen and Dudhia, 2001) are used to set up the model. The Rapid Radiative Transfer Model (RRTM) longwave radiation scheme is set. The radiation scheme provides atmospheric heating due to radiative flux divergence and surface downward longwave and shortwave radiation for the ground heat budget.

More details regarding the PBL and microphysics are given in Sect. 2.2.3.

The MM5 model has been set up to compute Sea Surface Temperature (SST) varying in time with 1-h output time resolution. The time step of output data has been set to 1 h.

2.2.2 Description of WRF

The Advanced Research WRF system (WRF-ARW V2.2) can be used as an alternative meteorological driver for MM5 in the air quality modelling. It is considered by NCAR as the successor of MM5, since further development of MM5 will come to an end in favour of WRF.

The WRF-ARW system is a non-hydrostatic model (with a hydrostatic option) using terrain-following vertical coordinate based on hydrostatic pressure.

The terrestrial data sets for the WRF model are built using the NCEP GFS geographical data. These consist in global data sets for soil categories, land use, terrain height, annual mean deep soil temperature, monthly vegetation fraction, monthly albedo, maximum snow albedo and slopes.

The initial resolution used for implementing terrain data in the proposed study is based on the 30 s database, as in MM5. The vertical discretization involves 24 levels up to about 20 km. The WRF-ARW system is suitable for a broad spectrum of applications across scales ranging from meters to thousands of kilometres.

The model is set up using single-moment 6-class microphysics scheme (WSM6) containing ice, snow and graupel processes, vapour, and rain (mixed-phase processes, appropriate for the analyzed range of spatial horizontal resolutions finer than 5 km, Hong and Lim, 2006). It uses the Noah land surface model scheme (Chen and Dudhia, 2001) with soil temperature and moisture in four layers, fractional snow cover and frozen soil physics and provides heat and moisture fluxes for the PBL. The PBL Yonsei University (YSU) scheme is used to set up the model (Hong et al., 2006). The radiation is calculated by the RRTM scheme (Mlawer et al., 1997). More details regarding the PBL and microphysics is given in Sect. 2.2.3.

The WRF model has been set up to compute SST varying in time with 1-h output

time resolution. In Table 2 an overview is given of the selected parameters in WRF and MM5.

2.2.3 Main differences between MM5 and WRF parameterization

A minimum set of physics components are required to create meteorological parameters, which are used by the air chemistry model to calculate gas and aerosol concentrations in space and time. These components are radiation, boundary layer and land-surface model, convective parameterization (detrainment, entrainment, moist updrafts and downdrafts), subgrid eddy diffusion, and microphysics (hydrometeos, i.e. water vapor, cloud water, rain, cloud ice, snow, and graupel).

To employ the meteorological models, the models were set up with the parameterizations mentioned in Sect. 2.2.1 and 2.2.2. There are some differences in the model settings between MM5 and WRF. Below, we describe the main differences in parameterization between the two meteorological models.

Planetary boundary layer scheme (PBL)

The planetary boundary layer is defined as that part of the troposphere that is directly influenced by the presence of the earth's surface, and responds to surface forcings (evaporation, transpiration, heat transfer, terrain induced flow modification) with a timescale less than an hour.

The PBL turbulence is responsible for vertical sub-grid scale fluxes due to Eddy transports in the whole atmospheric column, not just the boundary layer. Thus when a PBL scheme is activated, explicit vertical diffusion is de-activated with the assumption that the PBL scheme will handle this process.

The PBL schemes determine the flux profiles within the well-mixed boundary layer and the stable layer. This provides the atmospheric tendencies of temperature and moisture (including clouds).

The top of the PBL is described by the critical Richardson number which is the value

ACPD
9, 2319–2380, 2009

of the gradient Richardson number below which air becomes dynamically unstable and turbulent. The Richardson number is used to indicate the dynamic stability and the formation of turbulence. The critical Richardson number is set to zero in YSU PBL scheme in WRF, which means that it depends only on the buoyancy profile. In the MRF PBL's scheme, used in MM5, the critical Richardson number is set to 0.5. The YSU PBL scheme is a successor of MRF scheme (Hong et al., 2006) and is a standard PBL option in WRF, also used in other studies (Kesarkar et al., 2007; Guerrero et al., 2008).

Microphysics

The microphysics is described by moisture schemes and includes explicitly resolved water vapour, cloud and precipitation processes. Two different schemes are used for moisture in MM5 and WRF. In MM5 the Simple-ice (Dudhia, 1989) scheme is applied in which three categories of hydrometeors are included: vapour, cloud water/ice and rain/snow. The cloud water and cloud ice as well as rain and snow are distinguished by temperature as the cloud ice or snow can only exist when the temperature is less than or equal to the freezing point. In WRF the six-class scheme (WSM6) is used. Vapour, rain, snow, cloud ice and cloud water are held in five different arrays and an additional hydrometeor is taken into account, namely, graupel along with its associated processes. Thus the WSM6 scheme includes the mixed-phase processes which result from the interaction between ice and water particles, such as riming that produces graupel or hail. The freezing/melting processes are computed during the fall-term substeps to increase accuracy in the vertical heating profile of these processes. The common solution used in both Simple-ice scheme and the WSM6 scheme is the separate treatment of ice and water saturation processes (NCAR/TN-468+STR, 2007).

2.3 Emission data

In this study we use the City Delta III project (http://aqm.jrc.it/citydelta) emission inventory, which has been used in recent studies (Vautard et al., 2007 and Thunis et al.,

2007).

The inventory contains emissions for the year 2000 at a municipality level for the Lombardy region (Italy) for each pollutant, fuel and source sector, sub-sector, activity and about 237 point sources. These municipality emissions have been spatially disaggregated on a 5×5 km grid (Gauss Boaga projection) covering the whole Lombardy region using land-use percentage of each municipality in the grid cell (Maffeis et al., 2002). A detailed description of the emission inventory can be found in Cuvelier et al., 2007.

3 Description measurement data sets

The meteorological parameters provided by MM5 and WRF are compared with the observations from the EMEP measurement station Ispra (Italy) and from monitoring stations of the ARPA Lombardia network. The aerosol concentrations calculated by CHIMERE are compared with the aerosol measurements from the same or closely located air quality monitoring sites of the EMEP (Ispra, Italy) and ARPA networks (Lombardy, Veneto). The names of the stations for which we have meteorological data and PM_{10} data available are: Ispra (45.48° lat, 8.63° lon), Cantu (45.74° lat, 9.13° lon), Erba (45.79° lat, 9.20° lon), Mantova (45.16° lat, 10.80° lon) and Castelnovo Bariano (45.03° lat, 11.29° lon), Sermide (45.01° lat, 11.29° lon).

To have a broader view on measured ozone concentrations for comparison purposes, additional air quality monitoring sites (not collocated with meteorological stations) are taken into account from ARPA network (Lombardy). The names of the stations are Osio Sotto (45.63° lat, 9.60° lon), Gambara (45.25° lat, 10.29° lon), Corte de Cortesi (45.27° lat, 10.00° lon), Marmirolo Fontana (45.12° lat, 10.44° lon), Lecco (46.00° lat, 9.28° lon), Varese (45.63° lat, 8.88° lon), Chiavenna (46.32° lat, 9.40° lon) and Milano (45.49° lat, 9.24° lon). All air quality monitoring sites are characterized as background stations (including urban and suburban background), which is essential for comparison with the regional scale modelling results. More details regarding the

ACPD
9, 2319–2380, 2009

different networks are given below.

3.1 EMEP measurement site Ispra

The EMEP measurement station at Ispra, Italy (8.6° E, 45.8° N) makes part of the Co-operative Programme for Monitoring and Evaluation of the Long-range Transmission of Air Pollutants in Europe (EMEP), which evaluates air quality in Europe by operating a measurement network, as well as performing model assessments (http://www.emep.int/). This EMEP station, situated at the eastern side of the Lago Maggiore at the foothills of the Alps, is located on the premises of the Joint Research Centre, Ispra (Italy). Concentrations of carbon monoxide (CO), ozone (O_3) and secondary aerosol precursors (SO_2, NO_x) are continuously monitored (http://ccu.jrc.it/). Daily aerosol samples are collected on quartz fibre filters to determine PM_{10} and $PM_{2.5}$ concentrations and chemical compositions ($SO_4^=$, NH_4^+, NO_3^-, black carbon). Rain water samples are also collected to assess the aerosol wet deposition. In addition, PM_{10} concentration, aerosol size distribution in the range 8 nm–10 μm, and aerosol absorption coefficient are continuously monitored.

One of the artefacts occurring with the main filter type (quartz) used by the Ispra EMEP station, is the evaporation of ammonium nitrate at higher temperatures. Temperatures exceeding 20°C cause complete NH_4NO_3 evaporation from the quartz filter, a loss of 100%; and a loss of about 25% for NH_4^+. Temperatures between 20 and 25°C could lead to a loss of 50% of the nitrate aerosol (Schaap et al., 2003, 2004). Therefore almost all reported summer NH_4NO_3 and NH_4^+ concentrations present only a lower limit, rather than a realistic concentration.

3.2 ARPA

Monitoring data of the ARPA networks (Agenzia Regionale per la Protezione dell' Ambiente) in Lombardy (http://ita.arpalombardia.it/ita/index.asp) and Veneto (http://www.arpa.veneto.it) are used for comparison of meteorological variables (temperature, rel-

ative humidity, precipitation, wind speed and wind direction) with MM5 and WRF calculated meteorological parameters, as well as PM_{10} and O_3 measured values with calculated model concentrations.

Air quality data from 4 monitoring stations of ARPA networks (3 from Lombardy and 1 from Veneto) collocated with meteorological monitoring stations are used in this work: Erba, Cantu, Mantova and Castelnovo Bariano.

On the monitoring site of Erba concentrations of carbon monoxide (CO), ozone (O_3) and secondary aerosol precursors (SO_2, NO_x) are continuously measured as well as PM_{10} levels (using TEOM with correction factors). In Cantu the PM_{10} concentrations are measured using beta absorption method and apart from this continuous data about CO, O_3 and NO_x are being collected. In Mantova (S. Agnese) only NO_2, NO, CO and PM_{10} (using TEOM with correction factors) are measured.

On the monitoring station of Castelnovo Bariano (ARPA Veneto) concentrations of secondary aerosol precursors (SO_2, NO_x) as well as PM_{10} are continuously measured, using respectively fluorescence, chemiluminescence and gravimetric methods. Hourly meteorological data (for validation purposes) for this monitoring station are not available on the website of ARPA Veneto. Therefore the supporting meteorological data were taken from the monitoring station Sermide (ARPA Lombardia) which is located in the distance of about 2.5 km from Castelnovo Bariano.

All of the stations used for the comparison of modelled O_3 concentrations with measurements are located in Lombardy. They operate within ARPA network and measure ozone concentrations using the UV absorption method.

4 Results

Firstly we evaluated the two meteorological datasets by comparing the calculated meteorological parameters with observations. Secondly we performed an evaluation of the impact of using two meteorological models in the CHIMERE model on calculated PM_{10} and O_3 concentrations.

ACPD
9, 2319–2380, 2009

4.1 Meteorology

The evaluation of the modelled meteorological datasets is based on the observations from 5 monitoring stations located in Lombardy, Italy: Ispra, Mantova, Cantu, Erba and Sermide, using data given by ARPA Lombardia network. The following meteorological parameters were evaluated: absolute temperature on the 2 m level (data available for all stations), wind speed and direction (data available for 2 stations), as well as relative humidity and rain (data for 4 stations). For the rain data both analysis of the time series and the cumulative profiles were performed. The calculated statistics are: BIAS error, root mean square error (RMSE), standard deviation (SD) and the coefficient of determination (*R* squared). For detailed description of the formulas used to calculate statistics see Appendix. The analysis was performed for the annual means (year 2005) with the focus on winter (January 2005) and summer (June 2005) mean.

4.1.1 Annual (2005) mean statistics

Absolute temperature at 2 m

Both models underestimate the observed annual mean temperature at most of the monitoring stations. The underestimation ranges from 3.2% (0.4˚C) for MM5 in Cantu, up to 23.6% (3.6˚C) for MM5 in Mantova. In general WRF model gives higher temperatures than MM5 and shows also some small overestimation for monitoring points in Ispra and Cantu (BIAS <5%, which is <0.5˚C). The RMSE is within the range of 2.3 to 4.3˚C for both models. Comparison between the RMSE values from the models and the standard deviation (SD) values of the observations shows for all cases the relation of RMSE<SD, which is one of the conditions for good quality modelling results (Barna and Lamb, 2000). *R* squared values are comparable for both models, see Table 3a.

ACPD
9, 2319–2380, 2009

Relative humidity

In Table 3b we find that the annual mean of the relative humidity (RH) values are overestimated by WRF for 3 monitoring stations: Mantova, Erba and Cantu. The WRF overestimations are below 5% of observed values (<3% of relative humidity, RH). For the monitoring point in Ispra WRF underestimates the observed mean value of RH of about 7%, which corresponds to a RH of 5.4%. MM5 overestimates the RH value for Mantova and underestimates for Erba, Ispra and Cantu. The overestimation for Mantova reaches 5.8% of the observed value, which corresponds to a RH of 3.9%. For the other stations the BIAS for MM5 results is below 5% of the observed values. WRF gives lower RMSE values than MM5, however the BIAS values are in general lower for MM5. For both models all RMSE values are below the appropriate observational SD values. WRF results show higher R squared values than the MM5 results for the most of monitoring stations.

Wind speed

The results for wind speed and direction can be evaluated only for 2 monitoring points (in Ispra and Mantova). Moreover, the wind data are largely missing for Mantova, for the winter period (January–March) and so the reliable statistically analysis of the results is ensured mainly for the summer period.

The annual mean value for wind speed is well reflected by both models for Ispra. WRF gives very low, positive BIAS values (<1%, 0.01 m/s), see Table 3c. MM5 underestimates the wind speed by 31% (about 0.8 m/s). RMSE values are: 2.3 m/s for WRF and 1.9 m/s for MM5. However both models overestimate largely the wind speed for Mantova, for which the BIAS values are around 500% (~2 m/s) and RMSE values are 2.8 m/s for WRF and 2.6 m/s for MM5. All RMSE values (also for Ispra) are above the level of the SD of observed wind speeds. R squared values are very low.

The Po valley area is characterized by low wind speeds (stagnant conditions), which are difficult to simulate with the prognostic meteorological models such as MM5 (Dosio

ACPD
9, 2319–2380, 2009

et al., 2002; Minguzzi et al., 2005; Carvalho et al., 2006; Stern et al., 2008).

Wind direction

Both models do not reproduce well the annual mean wind direction (see wind roses in Fig. 2). When wind speeds are weak, wind direction fluctuates a lot, which is very difficult for the meteorological models to simulate. The BIAS values show the underestimation of the wind direction for Ispra (of 37–40%, which is about 105–110°) and an overestimation for Mantova (of about 210–220%, which is about 112–119°). Also the RMSE values are large and comparable between the models, for both monitoring points (about 140° for Ispra and 160° for Mantova). Moreover, they are much higher than the appropriate SD values. *R* squared values are close to zero, see Table 3d and Fig. 2.

Rain

The error measures calculated for the annual means (for time series) show that WRF overestimates (1.8 to 13.2%) and MM5 underestimates (11 to 20.9%) the amount of rain for 3 monitoring points (apart from Sermide). For Sermide both models show an overestimation (WRF 23%, MM5 around 3%). The RMSE values fall in the range of about 0.07–0.1 cm and are higher for WRF. All the RMSE values are higher than the appropriate SD values of observations. SD values calculated from the WRF results reflect better the variability of observations. *R* squared values are close to zero, see Table 3e.

The analysis of the annual cumulative profiles in Table 3f, shows that in general the BIAS error is lower for MM5. WRF usually overestimates the amount of rain (14–38% of observed values, which is about 6–10 cm). Only for the Ispra monitoring station the BIAS from WRF is negative and smaller than from MM5 (respectively, −3.7% and −22.8%, which is 1.3 and 8 cm). The MM5 model underestimates the rain for Ispra and Erba and overestimates for Cantu and Sermide. The RMSE values calculated from

ACPD
9, 2319–2380, 2009

the cumulative profiles are within the range from 2.7 cm (Ispra) to 12.5 cm (Sermide) for WRF and from 6.1 cm (Sermide) to 9.8 cm (Ispra) for MM5. In all cases the RMSE values are smaller than the level given by SD of observations. However, the variability of the rainfall cumulative curve is overestimated by WRF in all monitoring points.

4.1.2 Winter (January 2005) mean statistics

Absolute temperature at 2 m

For the winter period both models underestimate the mean temperature of about 31–68.6% (which corresponds to 0.7–2.1°C) for Sermide and Mantova (and Ispra for MM5). For Erba and Cantu (and Ispra for WRF) models show an overestimation of the mean temperature ranging from 12.3% (0.3°C) for MM5 in Erba up to about 300% (1.8°C) for WRF in Cantu. In general WRF output gives higher mean temperature values for the modelled winter period than MM5. The RMSE values are within the range from 2 to 4.4°C for both models and are generally lower than standard deviation values of observations (apart from MM5 results for Mantova). Analyzing the R squared values in Table 3a, WRF performed better than MM5 in the winter period.

Relative humidity

In Table 3b, the modelling results from the WRF model show an underestimation of the winter mean values of relative humidity varying from 4% (3.4% of RH) for Mantova, up to 12.9% (about 9.7% RH), for Ispra. Only for the monitoring station in Cantu the results from WRF show small overestimation of about 2% of observed values (1.3% of RH). MM5 results underestimate the observations. The BIAS values are higher than for WRF and vary from 9.1% (7.7% of RH) for Mantova, up to 17.2% (11.3% of RH) for Erba. The RMSE values range from 10.3% (WRF, Mantova) to 30.7% (MM5, Ispra) and are generally lower for WRF. For WRF all values of RMSE are lower than the standard deviation values of observations. WRF results show also higher R squared values than

the MM5 results.

Wind speed

The comparison of the results of wind speed and wind direction calculations by MM5 and WRF could be performed only for 1 monitoring point (in Ispra). WRF model overestimates the wind speed at this station by 23.4% (0.6 m/s) while the MM5 model shows underestimation of 30.6% (0.8 m/s). RMSE value is larger for WRF (2.8 m/s) in comparison to MM5 (2 m/s). Both RMSE values are much larger than the standard deviation of observations (which is 0.7 m/s). *R* squared values vary between 0.22 (for MM5) to 0.43 (for WRF), see Table 3c.

Wind direction

Wind roses for Ispra monitoring station show that both models do not reproduce well the observed wind direction during the winter period. The wind direction is underestimated. The error values are similar as for the annual analysis, see Table 3d.

Rain

The analysis of the rainfall time series from January in Table 3e, shows that WRF overestimates the amount of rain when compared to the 4 stations. MM5 shows an overestimation for Ispra and Sermide and an underestimation for Cantu and Erba. The value of the BIAS error is lower than 50% for most of the measurement stations. However, for Sermide it reaches very high values, especially for WRF results – of about 480% (0.65 mm). MM5 gives BIAS of 155.4% (0.21 mm). High error value given by WRF for Sermide is reflected also by RMSE value and by large overestimation of the observations variability. *R* squared value is close to zero apart from the MM5 output for Sermide where it reaches 0.36.

The analysis of the winter cumulative profiles shows similar results as for time series. Rainfall is overestimated for all stations by WRF but especially high values of errors

ACPD
9, 2319–2380, 2009

were calculated for the monitoring point in Sermide. The variability of the observational data set is largely overestimated for Sermide by both models, see Table 3f.

The high error values given by WRF for Sermide are caused mainly by the rainfall forecasted by WRF, which is 2.39 cm on the 1st of January, at 02:00 h LST and then, about the same amount of rain between the 18 (17:00 LST) and 19 (09:00 h LST) of January. Observational data show the first rainfall on the 5th of January (09:00 h) which is 0.02 cm and reach the amount of only 1 cm by the end of the month. WRF output calculates 5.82 cm of rain and MM5 about 2.6 cm of cumulated rainfall for January.

4.1.3 Summer (June 2005) mean statistics

Absolute temperature at 2 m

The mean temperatures modelled by both MM5 and WRF for the summer period are lower than the observation values for all stations. The underestimation ranges from 1.6% (0.4°C) for WRF in Ispra up to 17.4% (4.5°C) for MM5 in Mantova. RMSE values vary from 2°C (WRF, Sermide) to 4.9°C (MM5, Mantova) and are lower than the standard deviation of observations. The results from both models show similar *R* squared levels (Table 3a).

Relative humidity

The BIAS values for the relative humidity and the summer period show similar tendency for both models, see Table 3b. The mean summer values of the relative humidity are overestimated for the most of the monitoring stations. The BIAS values are in these cases within the range of 9.7% (5.6% of RH, in Erba, for MM5) up to 18.9% (10.6% of RH, in Cantu, for WRF). Only for Ispra both models show an underestimation ranging from 4.5% (3.2% of RH, for MM5) to 8% (5.7% of RH, for WRF). The BIAS values are generally lower for MM5. The RMSE values are within the range of 12% (in Mantova for WRF) to 16.9% of RH (in Ispra, for WRF) and are below the appropriate standard

ACPD
9, 2319–2380, 2009

deviation values. WRF results show higher *R* squared values than the MM5 results.

Wind speed

The pattern of error measurements for the wind speed and the summer period is similar to the results of the annual analysis. The mean value of the wind speed is well reflected by both models for Ispra monitoring station. The MM5 model underestimates the wind speed of 11.6% (0.2 m/s). WRF overestimates the wind speed by 12.7% (about 0.2 m/s). RMSE values are: 1.8 m/s for WRF and 1.3 m/s for MM5. Both models overestimate largely the wind speed values for Mantova, for which the BIAS values are around 400% (~2 m/s) and RMSE values are 2.7 m/s for WRF and 2.2 m/s for MM5. All RMSE values (also for Ispra) are above the level of the SD of observed wind speeds. *R* squared values are very low, see Table 3c.

Wind direction

Similar to the analysis for the whole year and the winter period, wind roses for Ispra and Mantova monitoring stations show that both models do not reproduce well the observed wind direction during the summer. The error indicators show similar values as for the annual analysis (Table 3d). The wind direction is underestimated for Ispra and overestimated for Mantova.

Rain

In the summer period, the analysis of the rainfall time series in Table 3e, shows for all monitoring points an overestimation which varies from 2.2% (0.02 mm) for MM5 in Ispra up to 202.5% (1.4 mm) for MM5 in Erba. The RMSE values are relatively high and exceed also the appropriate SD values for observations (apart from MM5 in Sermide). *R* squared values are close to zero.

The statistics for the cumulative profiles of the rainfall show lower BIAS values given by WRF output for the most of the monitoring points (apart from Sermide). Both models

ACPD
9, 2319–2380, 2009

overestimate the cumulative rainfall in almost all cases (apart form MM5 for Ispra). The highest error values appear for Erba monitoring station, where the BIAS values are about 164.7% (which is about 3.6 cm, for WRF) and 166.4% (about 3.7 cm, for MM5). Low error values are given for Ispra and Cantu monitoring points by WRF (BIAS of 12.7–21.7%, which is about 0.5–0.6 cm) and for the station in Sermide, by MM5 (BIAS of 3.8%, which is about 0.03 cm). RMSE value is higher than the SD of observations and the variability of the cumulative rainfall is overestimated in almost all cases. *R* squared varies within the range of 0.73 to 0.92 and is higher for MM5 in most of cases, see Table 3f.

4.1.4 Summary meteorological statistics

Summarizing the analysis of the annual averaged statistics shows that the temperatures are mainly underestimated (less by WRF) and the values of relative humidity are in general overestimated (less by MM5). WRF output follows better the hourly pattern of relative humidity. The wind speed is well reproduced for Ispra monitoring site (especially by WRF) but is largely overestimated by both models for Mantova (less by MM5). Both models do not reproduce well the wind direction. The rainfall is in general overestimated however the MM5 output shows lower rainfall values.

For the winter period WRF gives higher temperatures. The relative humidity is underestimated by both models however – less by WRF. For both of these parameters WRF results show generally higher *R* squared values than MM5 results. Both models do not reproduce well the observed wind field during the winter period. The wind speed values are overestimated by WRF and underestimated by MM5. However, WRF output follows better the hourly pattern of wind speed (higher *R* squared values than MM5). The rainfall is in general overestimated, mainly by WRF.

In the summer period both models underestimate the temperature and have similar *R* squared values, although WRF gives smaller error values. The relative humidity is mainly overestimated. WRF results show higher *R* squared values than MM5 for this parameter. The wind speed is well reproduced for Ispra monitoring site but is

largely overestimated by both models for Mantova (less by MM5). Both models do not reproduce well the wind direction. The rainfall is in general overestimated, although MM5 output shows higher R squared values.

4.2 Aerosols and ozone

In this section the impact of using two different meteorological models, MM5 and WRF in the CHIMERE model, on calculated PM_{10} and O_3 (ozone) concentrations is presented for January and June 2005.

4.2.1 Calculated PM_{10} concentrations with MM5 and WRF meteorology for January 2005

Aerosols formation is non-linear dependent on meteorological parameters, such as relative humidity, temperature, and removal processes (e.g. precipitation), which determine how aerosols are dispersed and transported over distance. Therefore for the comparison of calculated PM_{10} concentrations we selected those stations for which we have also meteorological data available. The combination of having PM_{10} measurement data together with meteorological data, allows us to understand better the PM_{10} profile.

For both simulations, using MM5 and WRF meteorology (CHIMERE/MM5 and CHIMERE/WRF), the model underestimates on average the observed PM_{10} concentrations for the five stations by a factor 2 and 3.2 for January respectively, see Table 4. Analyzing the calculated PM_{10} concentrations for the stations, we find that CHIMERE/MM5 shows an underestimation in PM_{10} for the Ispra station by a factor 1.3. Very high PM_{10} concentrations are observed at the beginning of the month for Mantova, leading to a monthly mean measured value of 207 $\mu g/m^3$, resulting to an underestimation of the model by a factor 3 (CHIMERE/MM5) and 6 (CHIMERE/WRF) for this station. These values are caused by fireworks at the beginning of the month (ARPA Lombardy, personal communication, 2008). Emissions from fireworks are not included

in our emission inventory. However, from the second half of the week onwards for Mantova, we find that the model underestimates PM_{10} by a factor 1.1 to 2.1 for both the simulations (CHIMERE/MM5 and CHIMERE/WRF). Excluding Mantova form the analysis shows a significant improvement of the results. PM_{10} concentrations are for the four stations underestimated on average by a factor 1.4 (CHIMERE/MM5) and 2 (CHIMERE/WRF).

As shown above, differences in calculated and observed PM_{10} concentrations are also found for the EMEP measurement station at Ispra (I). For this station we have to our disposal surface concentrations of $SO_4^=$, NO_3^-, NH_4^+, organic carbon and black carbon, which allows us to compare these aerosol species with model calculated values and allows us to determine which of the aerosol species is responsible for the discrepancy between observed and calculated aerosol concentrations.

Comparing NO_3^- aerosol (9.31 $\mu g/m^3$) and NH_4^+ (4.21 $\mu g/m^3$) for Ispra, we found that CHIMERE/WRF is in good agreement with the observations, see Table 5. CHIMERE/MM5 overestimates the observed NO_3^- aerosol concentrations by a factor of 1.4, while NH_4^+ calculated concentrations are in good agreement with the observations.

$SO_4^=$ is underestimated by a factor 2 (CHIMERE/MM5) and 1.5 (CHIMERE/WRF) when compared to the monthly mean observed value (3.83 $\mu g/m^3$). The wintertime underestimation of sulphate concentrations has been reported by previous studies and is possibly due to the insufficient of oxidation chemistry in the model (Jeuken, 2000; Kasibhatla et al., 1997).

The large underestimation of PM_{10} could be related to the underestimation of black carbon and organic carbon. Our model gives the sum of organic carbon (OC), elemental carbon (EC) and anthropogenic dust. Analysing the sum of OC, EC and anthropogenic dust, denoted as PPM, we see that the model underestimates for January the measured PPM by a factor of around 3 and 4 for CHIMERE/MM5 and CHIMERE/WRF, respectively, see Table 5. A possible explanation for this large underestimation is related to frequent wood burning for heating purposes in northern Italy in winter time.

ACPD
9, 2319–2380, 2009

Observations show that organic carbon has a significant contribution to the PM_{10} mass for Ispra (46%), with 29.8 $\mu g/m^3$. Elemental carbon contributes with 10% to PM_{10} mass (5.1 $\mu g/m^3$), and dust contributes with 2.5% to the total PM_{10} mass (1.4 $\mu g/m^3$).

Uncertainties in the emission factors for EC and OC in the emission inventory including unaccounted sources, which contribute to the underestimation of EC and OC in the inventory could be held responsible for the underestimation of PM_{10} in a winter period, as discussed by Schaap et al., 2004. The underestimation may be also related to the overestimation of the relative humidity by the two meteorological models (Sect. 4.1.4), which suppress the local re-suspension of anthropogenic dust.

4.2.2 Differences in calculated PM_{10} concentrations between CHIMERE/MM5 and CHIMERE/WRF for January

Our analysis of calculated PM_{10} concentrations for the five stations in January shows that modelled mean PM_{10} values between CHIMERE/MM5 and CHIMERE/WRF are different. The calculated PM_{10} values for CHIMERE/MM5 are on average a factor 1.6 higher than CHIMERE/WRF. Analyzing the monthly mean PM_{10} concentration for January for Ispra (CHIMERE/MM5), we find a concentration around 43.2 $\mu g/m^3$. CHIMERE/WRF calculates a monthly mean PM_{10} concentration of 26.6 $\mu g/m^3$ for Ispra, see Table 4. The differences in PM_{10} concentrations for January are on average around 10 $\mu g/m^3$ (not shown), with the exception of the period 14–18 January, where a large difference in calculated PM_{10} between the two simulations is found, see Sect. 4.2.3 for a detailed the explanation for this.

To understand the differences in PM_{10} between CHIMERE/MM5 and CHIMERE/WRF, we analyse the PBL heights and the related sensible and latent heat fluxes (SHF and LHF respectively) for the five different locations, for which we compare the PM_{10} calculated concentrations. The sensible heat flux (dry) and latent heat flux (moist) are provided by the land surface model. The reason why we analyze first the SHF and LHF is that these parameters provide the heat fluxes to the PBL

scheme which stimulates the turbulence in the boundary layer and determines the height and temporal profile of the PBL and the resulting vertical aerosol distribution.

The LSM model applied in MM5 and WRF is Noah, therefore surface and latent surface heat fluxes should be similar.

For the five different locations we observe similar SHF. On average the monthly mean SHF with MM5 is $-8.0\,W/m^2$ and with WRF $-6.9\,W/m^2$. However, for the LHF larger differences are observed between MM5 and WRF, which is in general $10.2\,W/m^2$ for WRF and $5.7\,W/m^2$ for MM5.

The underlying reason for these differences in LHF, is that the shortwave incoming radiation at the surface between MM5 and WRF is different. Overall more shortwave incoming radiation is observed by MM5. The downward shortwave radiation is a source of energy for the soil. More incoming shortwave radiation and the availability of moisture at the surface will stimulate the heat and moisture transport away upward from the surface (Stull, 1988). The difference in shortwave radiation between MM5 and WRF is a result of the difference in cloud cover. Analyzing the cloud attenuation between the two meteorological models, we observe that in general MM5 shows less cloud attenuation than WRF does, which results in more incoming radiation by MM5. This is due to the difference in microphysics scheme. The number of hydrometer categories in WSM6 (vapour, cloud water, cloud ice, rain, snow, graupel) is larger than in the Simple Ice scheme (vapour, cloud water/ice, rain/snow), this leads to more cloud liquid water and more rain fall (Hong et al., 2006).

More cloud attenuation by WRF, results is more cloud liquid water content by WRF (and more rain by WRF as described in Sect. 4.1.2). This has an impact on the latent heat flux by WRF, which is in general almost a factor 2 higher as mentioned earlier.

This larger flux of latent heat by WRF is responsible for the higher PBL heights. On average, the PBL height by WRF for the 5 stations at noon is around 270 m, while by MM5 97 m. This is more than a factor 2.8 difference. This difference in PBL height is responsible for the differences in aerosol concentrations between CHIMERE/WRF and CHIMERE/MM5. The vertical mixing with WRF meteorology is better, because of

the higher PBL height, which leads to lower aerosol concentrations at ground level than with MM5 meteorology as mentioned before. We did not have observational data to our disposal, to compare calculated PBL heights by MM5 and WRF with measurements. However, comparing the calculated PBL heights between MM5 and WRF, gives us the possibility to understand the differences in calculated aerosol concentrations.

4.2.3 Episode of large difference in PM_{10} concentrations between CHIMERE/MM5 and CHIMERE/WRF

In Sect. 4.2.2 is mentioned that a large difference in calculated PM_{10} concentrations between CHIMERE/MM5 and CHIMERE/WRF is observed for the period 14–18 January for Ispra. In this section we give the explanation for this large difference in PM_{10}.

Analyzing the temporal profile of PM_{10} concentrations for January for CHIMERE/MM5 and CHIMERE/WRF, we observe maximum PM_{10} values of 90 $\mu g/m^3$ by CHIMERE/MM5, whereas CHIMERE/WRF calculates a maximum of 45 $\mu g/m^3$. This large difference in calculated PM_{10} concentrations cannot be explained by the difference in PBL scheme alone.

This large difference in PM_{10} calculated values is related to the difference in calculated NO_3^- concentrations by CHIMERE/MM5 (33 $\mu g/m^3$) and CHIMERE/WRF (16 $\mu g/m^3$) for this period. The underlying reason for the higher NO_3^- aerosol concentrations by CHIMERE/MM5 can be explained by the absence of cloud liquid water (CLW) in MM5 for that period (observed in WRF). As described before (Sect. 4.2.2) the microphysics scheme in WRF produces more CLW than in the Simple Ice scheme, because of the number of hydrometer categories in WSM6 (Hong et al., 2006). The oxidation of SO_2 in cloud liquid water by H_2O_2 is very fast and is an important source of sulphate aerosol formation (Pandis and Seinfeld, 1989; Seinfeld and Pandis, 1998 and references herein), see reactions below:

$$HSO_3^- + H_2O_2 \leftrightarrow SO_2OOH^- + H_2O \quad \text{(R1)}$$

$$SO_2OOH^- + H^+ \rightarrow H_2SO_4 \quad \text{(R2)}$$

ACPD
9, 2319–2380, 2009

SO_2 concentrations during this period with CHIMERE/WRF drop to an average of 0.75 ppb while CHIMERE/MM5 calculates an average of 5.0 ppb during this period. Mean H_2O_2 concentration for the CHIMERE/WRF is around 0.02 ppb, whereas CHIMERE/MM5 a mean of 0.07 ppb is calculated for that period. CHIMERE/WRF calculates a mean concentration of $SO_4^=$ of 5.5 μg/m^3, while CHIMERE/MM5 calculates a mean of 2.0 μg/m^3 $SO_4^=$ for that 5 days period. CHIMERE/MM5 calculates lower $SO_4^=$ concentration, because SO_2 is not oxidized by H_2O_2 into $SO_4^=$ as there is no CLW observed by MM5 for that period. Due to the presence of CLW in the WRF meteorology, SO_2 is oxidized by H_2O_2 into SO_4 aerosol.

As mentioned before, CHIMERE/WRF calculates a mean NO_3^- concentration of 16 μg/m^3 for the period 14–18, whereas for CHIMERE/MM5 a mean concentration of 33 μg/m^3 is calculated. These large differences in NO_3^- aerosol contribute to the differences in PM_{10}.

The difference between the two simulations in NO_3^- calculations can be explained by the reaction of the sulphate aerosol with ammonia. If sufficient ammonia is available to neutralize all sulphate, the residual amount of ammonia can neutralize nitric acid to form the ammonium nitrate aerosol. We have seen that CHIMERE/MM5 does not produce much $SO_4^=$ as CHIMERE/WRF does. This means that the ammonia can react with the nitric acid to form the nitrate aerosol, leading to a higher NO_3^- concentration than CHIMERE/WRF, causing higher PM_{10} values between the 14 and 18 January than CHIMERE/WRF.

4.2.4 Spatial distribution of PM_{10} calculated concentrations by CHIMERE/MM5 and CHIMERE/WRF for January

Figure 3 shows the monthly mean spatial distribution of the PM_{10}. Large differences between the model simulations using MM5 and WRF are found. For CHIMERE/MM5 (Fig. 3a) the model calculates a PM_{10} concentration around 40–50 μg/m^3 for a large part over the Po valley, with elevated levels for the Milan city, up to 105 μg/m^3.

ACPD
9, 2319–2380, 2009

In Fig. 3b, CHIMERE/WRF shows a much lower PM_{10} concentration over the Po valley area than CHIMERE/MM5 (on average a factor 2 lower) and a concentration for the Milan city of 59 $\mu g/m^3$. These differences are due to the difference in LHF and the resulting PBL heights caused by microphysics as described in Sect. 4.2.2. A sensitivity analysis showed that changing only the PBL scheme in WRF from YSU into MRF, does not improve the calculated PM_{10} concentrations for January.

Another important parameter responsible for the surface heat fluxes could be related to the choice of the land surface model.

We performed a sensitivity analysis by changing the Noah LSM scheme in WRF by the 5-layer soil temperature model and the YSU PBL with the MRF.

The PM_{10} spatial distribution and concentrations for this simulation improve in Fig. 3c. For the Po valley area PM_{10} concentrations are on average around 35–40 $\mu g/m^3$, which is up to a factor of 1.6 higher than the simulation using WRF meteorology with the Noah land surface model and closer to the concentrations of CHIMERE/MM5 (CHIMERE/MM5 20% higher) and correspond better to the observations in the Lombardy region. For the Milan city a monthly mean concentration of 79 $\mu g/m^3$ is found, which is a factor 1.3 higher than with Noah LSM and is closer to CHIMERE/MM5. For the five stations, the PM_{10} concentrations are on average 41% higher than with Noah LSM and YSU PBL.

As described above, the choice of LSM has an impact on the heat fluxes and the resulting PBL heights, the vertical mixing and therefore in the aerosol concentration. The underlying reason for the improvement in PM_{10} concentrations is related to the change in PBL height with the 5 layer soil temperature LSM+MRF PBL scheme in respect to the PBL height with the Noah LSM. When we analyze for the stations the heat fluxes we see that the SHF with the 5-layer soil moisture LSM are on average a factor 2 lower than with the Noah LSM; on average $-13.6\,W/m^2$ with WRF 5-layer soil temperature and MRF PBL, while with Noah LSM an average of $-6.9\,W/m^2$ is calculated. However, LH fluxes are on average $2\,W/m^2$ higher using the 5-layer soil temperature LSM than with Noah LSM.

ACPD

9, 2319–2380, 2009

Analyzing the resulting PBL heights for the 5 stations using the 5-layer soil temperature LSM, we see that the PBL height at noon for Ispra, Erba and Cantu are a factor 2 lower than when the Noah LSM is used and are closer to the PBL heights calculated by MM5. This results in reducing the vertical mixing in the first layers, leading to higher aerosol concentrations at ground level.

When we change the Noah LSM scheme in our WRF pre-processing for the 5-layer soil temperature model and keep the YSU PBL scheme, calculated PM_{10} concentrations for January 2005 increase by 30% in respect to the simulation using Noah LSM.

4.2.5 Calculated PM_{10} concentrations with MM5 and WRF for June

In Table 6 we analyse the model results of the calculated monthly PM_{10} concentrations for June 2005 and compare them with observations for 5 stations in the Lombardy region.

For both model simulations the PM_{10} concentrations are in better agreement with the observations than in January. The model mean calculated concentrations by CHIMERE/MM5 (on average 29.9 $\mu g/m^3$) and CHIMERE/WRF (on average 30 $\mu g/m^3$) agree well with the observations (29.2 $\mu g/m^3$).

Calculated $SO_4^=$, and NH_4^+ concentrations are in good agreement with the observations, see Table 7. $SO_4^=$ CHIMERE/MM5 (5.00 $\mu g/m^3$) and CHIMERE/WRF (5.65 $\mu g/m^3$) are in a good agreement with the observations (5.38 $\mu g/m^3$).

NO_3^- aerosol by CHIMERE/WRF is overestimated by a factor 1.7 and the monthly mean concentration by CHIMERE/MM5 is overestimated by a factor 1.3 when compared to the observations. The calculated monthly mean NH_4^+ concentrations by CHIMERE/MM5 and CHIMERE/WRF are in good agreement with the observations. At temperatures between 15°C and 20°C, NH_4^+ and NO_3^- evaporate partially from the quartz filter, which was used in 2005 for the aerosol measurements at the EMEP station in Ispra. However, temperatures exceeding 20°C cause NH_4^+ and NO_3^- to evaporate completely from the quartz filter (Schaap et al., 2003a, b), a loss of 100% for NO_3^-, and

a loss of about 25% for NH_4^+ (De Meij et al., 2006). As daily temperatures at the EMEP station in June 2005 were above 20°C, less NH_4^+ and NO_3^- is found on the filters and therefore the measured NH_4^+ and NO_3^- must be considered as a lower limit.

Analysing the PPM (sum of EC, BC and dust), we see that the model underestimates the measured PPM by a factor 2.8 (CHIMERE/MM5) and 2.5 (CHIMERE/WRF). A possible explanation for this is related to the emissions factors applied for BC and EC in the emission inventories, as described before.

The differences in PM_{10} concentrations between the two model simulations are small, which is not the case for January as described before. The underlying reason for this is that difference in the heat fluxes between MM5 and WRF are not that large as seen for January; SHF by WRF is 7% higher, LHF by WRF is 9% lower when compared to the heat fluxes calculated by MM5.

These smaller differences in the heat fluxes result in the small differences in PBL heights for the five different stations. The PBL heights, using MM5 and WRF, both with Noah LSM scheme, are on average ±1407 m (MM5) and ±1464 m (WRF) for June for the five stations at 2 pm. These small variations in the PBL heights will not affect the vertical mixing in the first layers of the model and therefore not invoke a large difference in aerosol distribution between the two model simulations.

4.2.6 Sensitivity analysis of PM_{10} calculations for January

Our model simulations using MM5 and WRF meteorology showed underestimations in PM_{10} concentrations for January 2005. These could be related to the uncertainties in the emission inventories and the lack of natural and anthropogenic sources of PM. However, we observed also large differences in calculated aerosol concentrations between model simulations using MM5 and WRF meteorology, while the emission input does not change.

In this section we explain that the latter difference is related to the parameterizations in the meteorological pre-processing.

In Sect. 4.2.4 we have seen that changing the LSM in WRF from Noah to the 5-layer soil temperature model and the PBL scheme from YSU into MRF, increase the calculated PM_{10} concentrations on average to 41% for the 5 stations.

We explain that the underlying reason for is related to the change in PBL height, which is in general lower with the 5 layer soil temperature LSM for January than with Noah LSM. A sensitivity analysis showed that changing only the PBL scheme in WRF from YSU into MRF, does not improve the calculated PM_{10} concentrations for January.

Another sensitivity analysis showed that changing the LSM model in MM5 from Noah to the 5-layer soil temperature model, sensible heat and latent heat fluxes change and to some extent the resulting PBL heights.

On average, the SHF for the 5 stations using the 5-layer soil temperature model is almost a factor 2 lower, i.e. $-14.6\,W/m^2$ (which corresponds with the average SHF using 5-layer soil temperature model in WRF, $-13.6\,W/m^2$), while with the Noah LSM, SHF is on average $-8.0\,W/m^2$, as described in Sect. 4.2.2. However, LHF goes up from $5.7\,W/m^2$ (Noah) to $11.2\,W/m^2$. This results in that the PBL height does not change as much as seen between MM5 and WRF and therefore aerosol concentrations does not change much (on average $2\,\mu g/m^3$ for the Po valley area).

When the Simple Ice microphysics scheme in the MM5 simulation is changed for the Mixed Phase microphysics scheme, we see that the monthly mean PM_{10} concentrations are lower, up to 20%. The underlying reason for this is that with the Mixed Phase scheme, more cloud liquid water is calculated by the model than with the Simple Ice scheme, which is responsible for lower NO_3 aerosol peak values and the resulting PM_{10} values as described in Sect. 4.2.3.

4.2.7 Calculated O_3 concentrations with CHIMERE/MM5 and CHIMERE/WRF for June

In Table 8 the monthly mean O_3 calculated values by CHIMERE/MM5 and CHIMERE/WRF are given for 9 background stations, together with the observations and the correlation coefficients.

Overall the monthly mean O_3 values by CHIMERE are overestimated on average by a factor 1.3 for both using MM5 and WRF meteorology and the correlation coefficients are in general higher by CHIMERE/MM5.

The underlying reason for the overestimations is related that CHIMERE/MM5 calculates a daily average NO_2 concentration of 8.6 ppb and CHIMERE/WRF a daily average of 6.8 ppb (sampled at 12:00 a.m. LST). This is a factor 3 and 2 higher, respectively, than the observed NO_2 concentrations at Ispra (3.0 ppb). The higher NO_2 concentrations calculated by the model result in higher O_3 concentrations during the day, because ozone is chemically formed by the oxidation process of volatile organic compounds (VOCs) in the presence of NO_x ($NO+NO_2$) and its formation is driven by the sunlight intensity.

We also observe that the minimum O_3 values are not well captured by the model, which indicates a weak O_3 titration by the model. The depletion of O_3 ($O_3+NO \rightarrow NO_2+O_2$) is important during the night time and early hours in the morning. The model calculates for Ispra an average O_3 daily minimum value (sampled at 02:00 LST in the morning) of 34.0 ppb by CHIMERE/MM5 and 41.1 ppb by CHIMERE/WRF, while the average daily minimum value for the observation is a factor 2 lower (18.3 ppb). For Marmirolo Fontana, the average measured daily minimum value is 18.0 ppb, while the calculated average daily minimum by Chimer/MM5 is 31.9 ppb and by CHIMERE/WRF 33.7 ppb.

Comparing the NO measured concentrations (0.49 ppb, sampled at 02:00 LST) with the model calculated concentrations, we find that the nighttime NO concentration by CHIMERE/MM5 and CHIMERE/WRF are underestimated by a factor 5 and 7, respectively. These low NO concentrations weaken the titration effect and result in higher O_3 values during the night calculated by the model. Measured O_3 values in the Po Valley area can drop to below 5ppb during the night due to the titration effect (http://ita.arpalombardia.it/ita/index.asp). These low O_3 concentrations are not calculated by the model.

In Fig. 4a and b, the monthly (June) mean O_3 concentrations by the CHIMERE model

are shown, using MM5 and WRF meteorology. In general the concentrations in the Po Valley area are similar. However we observe differences in O_3 values in the mountain regions, of around 6–9 ppb with a maximum up to 14 ppb. Analyzing the monthly mean wind direction and wind speed, we see that WRF monthly mean wind speed is 3 m/s, with a larger daily amplitude and frequency from south to north direction. The monthly mean wind speed by MM5 is 2 m/s, with lower daily velocity amplitude and a lower south–north frequency. The larger wind speed by WRF transports the O_3 from the Po valley area higher up over the mountains, resulting in higher O_3 concentrations over this area. A similar effect of larger wind speeds on O_3 concentrations over the Pre Alps has been observed earlier by Minguzzi et al. (2005).

For both the model simulations low O_3 values over the Milan city are calculated, due to the presence of high NO concentrations which are responsible for the night time depletion of O_3.

5 Summary and concluding remarks

The impact of two different meteorological models (MM5 and WRF) on PM_{10}, aerosols and O_3 calculations over the Po valley region (Italy) for January and June 2005 is investigated.

First we evaluate for January, June and annually the calculated meteorological parameters by MM5 and WRF (temperature, wind speed, wind direction, relative humidity and precipitation) with observations.

Overall we can say that the analysis of the meteorological modelling results shows that the performance of both models is similar in all tested periods however small differences are still noticeable. The temperatures are usually underestimated but in the most of cases within a BIAS range of 20% (−3°C), in relation to the observed values. RMSE varies from 2 to 4.4°C and is lower than the SD calculated from observations. WRF usually produces higher temperature averages than MM5. The relative humidity is mainly overestimated but the BIAS values, related to observations, do not reach the

level of 20%. RMSE changes from about 12 to 20% (only for January the range is larger: from ~10 to 31%) and the condition of $RMSE_{mod}$<SD_{obs}, is fulfilled in most of cases also for this parameter. WRF produces higher averages of relative humidity than MM5 during the winter period. The wind field is not well reproduced due to difficulties caused by very low wind speeds occurring in the Po Valley area (average observed wind speeds over all analyzed periods were below 1 m/s). Both models overestimate largely the wind speed values with the BIAS up to 2.7 m/s and RMSE varying from 1.3 up to 3.3 m/s. The WRF model usually produces higher wind velocities than MM5. Also the observed wind direction was not well reflected by the models. BIAS values change within the range of about |46–130°| and RMSE from 124 to 167°. The largest differences between the models in relation to the wind direction were noticed for stations located closer to mountains and/or lakes (like Ispra and Erba). The quantity of precipitation, according to statistics for the whole year, is reproduced by both models with the BIAS within the range of |3.7–38%| in relation to the observed values and the RMSE below the value of SD calculated from observations. For the particular periods (January and June) the error values are larger. The quantity of rain is in general overestimated. The WRF model produces more precipitation than the MM5.

This study evaluates the impact of using two different meteorological models with the CHIMERE model on aerosol and O_3 calculations for January and June 2005.

In general the model underestimates the observed PM_{10} concentrations by a factor 2 (with MM5 meteorology) and 3 (with WRF meteorology) for January 2005. NH_4^+ is in good agreement with the observations for the Ispra EMEP station for both the models, whereas NO_3^- using the MM5 meteorology is underestimated by a factor 1.4, but is in good agreement with observations using WRF. $SO_4^=$ is underestimated by a factor 2 and 1.5 by the model using MM5 and WRF, respectively. However, the sum of EC, OM and anthropogenic dust is underestimated from the observations by the simulation using MM5 (by a factor 3) and WRF (by a factor 4).

The difference in PM_{10} concentrations for January between CHIMERE/MM5 and CHIMERE/WRF is around a factor 1.6 (PM_{10} higher with MM5 meteorology). This

ACPD
9, 2319–2380, 2009

difference and the larger underestimation in PM_{10} concentrations by CHIMERE/WRF are related to the differences in PBL heights calculated by WRF meteorology. In general the PBL height by WRF meteorology is a factor 2.8 higher at noon in January than calculated by MM5. This could result in a better vertical mixing of the aerosols than CHIMERE/MM5, causing lower aerosol concentrations at the surface.

The underlying reason for the differences in PBL heights can be explained by the differences found in the latent heat flux, which is responsible for the profile of the PBL. The WRF meteorology calculates a monthly mean latent heat flux which is a factor two larger than MM5.

The explanation for these differences in LHF is that the shortwave incoming radiation at the surface between MM5 and WRF is somehow different. In general more shortwave incoming radiation is observed by MM5 as a result of less cloud cover by MM5, which is caused by the difference in the microphysics scheme in MM5 and WRF.

This difference in microphysics scheme helps us to explain also the difference in PM_{10} peak values, which are observed between the 14 and 18 January, as described in Sect. 4.2.3. In that section we explain that the presence of cloud liquid water (CLW) leads to the oxidation of SO_2 into $SO_4^=$ aerosol. The absence of CLW at certain periods by MM5 (when WRF calculates CLW) leads to the production of higher NO_3^- concentrations, and the resulting higher PM_{10} concentrations.

Changing the Noah LSM scheme in our WRF pre-processing for the 5-layer soil temperature model, calculated PM_{10} concentrations for January 2005 increase by 30% in respect to the simulation using Noah LSM.

For June the differences in PM_{10} concentrations between the model simulations using MM5 and WRF are small. Compared to the observations, the model simulation using MM5 and WRF meteorology corresponds well with the observations (29.2 $\mu g/m^3$). Analyzing the heat fluxes, the PBL height and PBL profile we observe small differences between the two meteorological models.

Analyzing the calculated O_3 values for June, we see that for both the simulations the model overestimates on average by a factor 1.3 the measured O_3 concentrations and

the correlation coefficients are in general higher by CHIMERE/MM5. The reason for the overestimation this is twofold. Firstly, the calculated NO_2 concentrations during the day by both CHIMERE/MM5 and CHIMERE/WRF are a factor 3 and 2 higher, respectively, than the observations. This could lead to an increase of O_3 production during daytime. Another possible explanation for the overestimation could be related to the O_3 titration during the night and early morning, which is not large enough in the model. NO is responsible for the depletion of O_3 during nighttime. The model calculates with both the meteorological models, NO concentrations which are a factor 5 (CHIMERE/MM5) to 7 (CHIMERE/WRF) lower than the observations. The higher O_3 concentrations over the mountains with WRF meteorology could be related to the higher daily and more frequent south to north wind speed during day time than by MM5, bringing the O_3 from the Milan area up to the mountains.

Similar differences in calculated O_3 concentrations were observed by Minguzzi et al. (2005). In this study the wind fields were varied, leading to higher ozone concentrations over the foothills of the Alps.

Underestimation of PM_{10} calculations is a common problem in air quality modelling (Van Loon et al., 2004; Schaap et al., 2007; Vautard et al., 2007; Stern et al., 2008). The underlying reason for this could be related to different factors contributing to the uncertainties in air quality modelling, such as uncertainties in the emission inventories, including the temporal and vertical distribution of the emissions (De Meij et al., 2006), the lack of natural and anthropogenic sources of PM (Schaap et al., 2004), the role of the gas and aerosol boundary conditions on calculated aerosol concentrations in de model domain (De Meij et al., 2007) and the uncertainties in the meteorological parameters, such as mixing height and temperature (Hongisto, 2005) and wind fields (Minguzzi et al., 2005).

In the Po valley, especially during winter time, stagnant weather conditions are observed. These meteorological conditions are responsible for high PM concentrations. Low wind speeds and low inversion heights are responsible for these stagnant conditions, which are difficult to simulate with the meteorological models such as MM5

ACPD
9, 2319–2380, 2009

(Dosio et al., 2002; Minguzzi et al., 2005; Carvalho et al., 2006; Stern et al., 2008).

This phenomenon was also encountered for the Milan city by the models in the City-delta exercise (http://aqm.jrc.it/citydelta, Cuvelier et al., 2006; Vautard et al., 2006).

This study showed the differences in meteorological parameters between two meteorological models over complex areas, especially during winter time periods. It shows how this affects the calculated gas and aerosol concentrations, which are non-linear dependent on meteorological conditions.

The challenging task for the future is to improve the models' capability to simulate meteorological parameters, such as wind speed, wind direction, heat fluxes over complex terrain with a higher accuracy. This will improve, together with a more accurate emission inventory, the calculated gas and aerosol concentrations, which are necessary for scientific studies and for policy making.

Appendix A

Definition of the statistical parameters used for the comparison between modelled concentrations and observed data.

$$\mathrm{SD}=\sqrt{\frac{\sum_{i=1}^{n}\left(y-\overline{y}\right)^2}{n}}$$

Standard deviation: a measure of the dispersion of the observed (calculated) values around the mean.

$$\mathrm{RMSE}=\sqrt{\frac{\sum_{i=1}^{n}(x-y)^2}{n}}$$

Root mean square error: a measure of difference between the model and the observations (measure of accuracy).

$$\text{BIAS} = \frac{\sum_{i=1}^{n} x - y}{n}$$

Measure of overestimation or underestimation.

$$\text{REL(BIAS)} = \frac{\text{BIAS}}{\overline{y}}$$

$$\text{REL(RMSE)} = \frac{\text{RMSE}}{\overline{y}}$$

$$R^2 = (\text{CORR})^2$$

Square of the correlation coefficient (indicates the linear relationship between model and observations).

y – observed value
$\overline{y}$ – mean of observed values
x – modeled value
n – number of observations

Acknowledgements. The authors would like to thank E. Chaxel for the WRF interface in CHIMERE, J. L. Monge and S. Potempski for the additional support of the code, S. Galmarini for the valuable discussions. Also thanks to A. R. P. A. Lombardy and Veneto for the PM_{10} and meteorological measurements. This work has been performed on the Beowulf Linux cluster of the Global Environment Monitoring Unit, Institute of Environment and Sustainability, JRC, Ispra (I).

References

Barna, M. and Lamb, B.: Improving ozone modeling in regions of complex terrain using observational nudging in a prognostic meteorological model, Atmos. Environ., 34, 4889–4906, 2000.

Bessagnet, B., Hodzic, A., Vautard, R., Beekman, M., Cheinet, S., Honeré, C., Liousse, C., and Rouil, L.: Aerosol modeling with CHIMERE – preliminary evaluation at the continental scale, Atmos. Environ., 38, 2803–2817, 2004.

Carvalho, A. C., Carvalho, A., Gelpi, I., Barreiro, M., Borrego, C., Miranda, A. I., and Pérez-Muñuzuri, V.: Influence of topography and land use on pollutants dispersion in the Atlantic coast of Iberian Peninsula, Atmos. Environ., 40, 3969–3982, 2006.

Chen, F. and Dudhia, J.: Coupling an advanced landsurface/hydrologymodel with the Penn State/NCAR MM5 modeling system, Part I: Model description and implementation, Mon. Weather Rev., 129, 569–585, 2001.

Colella, P. and Woodward, P. R.: The Piecewise Parabolic Method (PPM) for Gas-Dynamical Simulations, J. Comp. Physiol., 54, 174–201, 1984.

Cuvelier, C., Thunis, P.,Vautard, R., Amann, M., Bessagnet, B., Bedogni, M., Berkowicz, R., Brocheton, F., Builtjes, P., Denby, B., Douros, G., Graf, A., Honoré, C., Jonson, J., Kerschbaumer, A., de Leeuw, F., Moussiopoulos, N., Philippe, C., Pirovano, G., Rouil, L., Schaap, M., Stern, R., Tarrason, L., Vignati, E., Volta, L., White, L., Wind, P., and Zuber, A.: CityDelta: a model intercomparison study to explore the impact of emission reductions in European cities in 2010, Atmos. Environ., 41, 189–207, doi:10.1016/j.atmosenv.2006.07.036, 2007.

de Meij, A., Krol, M., Dentener, F., Vignati, E., Cuvelier, C., and Thunis, P.: The sensitivity of aerosol in Europe to two different emission inventories and temporal distribution of emissions, Atmos. Chem. Phys., 6, 4287–4309, 2006, http://www.atmos-chem-phys.net/6/4287/2006/.

de Meij, A., Wagner, S., Gobron, N., Thunis, P., Cuvelier C., and Dentener, F.: Model evaluation and scale issues in chemical and optical aerosol properties over the greater Milan area (Italy), for June 2001, Atmos. Res., 85, 243–267, 2007.

Derognat, C., Beekmann, M., Baeumle, M., Martin, D., and Schmidt, H.: Effect of biogenic volatile organic compound emissions on tropospheric chemistry during the Atmospheric Pollution Over the Paris Area(ESQUIF) campaign in the Ile-de-France region, J. Geophys. Res.,

108(D17), 8560, doi:10.1029/2001JD001421, 2003.
Dosio, A., Galmarini, S., and Graziani, G.: Simulation of the circulation and related photochemical ozone dispersion in the Po plains (northern Italy): comparison with the observations of a measuring campaign, J. Geophys Res., 107(D18), 8189, doi:10.1029/2000JD000046, 2002.
Dudhia, J.: Numerical study of convection observed during the winter monsoon experiment 10 using a mesoscale two – dimensional model, J. Atmos. Sci., 46, 3077–3107, 1989.
Dudhia, J.: A multi-layer soil temperature model For MM5, Preprints, The 6th PSU/NCAR Mesocale Model MM5 Users Workshop, Boulder, CO, USA, 1996.
Fuchs, N. A.: The mechanics of aerosols, Pergamon Press, London, UK, 1964.
Ginoux, P., Chin, M., Tegen, I., Prospero, J. M., Holben, B., Dubovik, O., and Lin, S.-J.: Sources and distributions of dust aerosols simulated with the GOCART model, J. Geophys. Res., 106, 20255–20273, 2001.
Ginoux, P., Prospero, J. M., Torres, O., and Chin, M.: Longterm simulation of dust distribution with the GOCART model: Correlation with the North Atlantic Oscillation, Environ. Modell. Softw., 19, 113–128, 2004.
Grell, G. A., Dudhia, J., and Stauffer, D. R.: A description of the fifth-generation Penn State/NCAR mesoscale model (MM5), NCAR Tech. Note TN-398+STR, 122 pp., 1994.
Grosjean, D. and Seinfeld, J. H.: Parameterization of the formation potential of secondary organic aerosols, Atmos. Environ., 23, 1733–1747, 1989.
Guelle, W., Balkanski, Y. J., Dibb, J. E., Schulz, M., and Dulac, F.: Wet deposition in a global size-dependent aerosol transport model, 2. Influence of the scavenging scheme on 210 Pb vertical profiles, surface concentrations, and deposition, J. Geophys. Res., 103(D22), 28875–28891, 1998.
Guerrero, P. J., Jorba, O., Baldasano, J. M., and Gasso, S.: The use of a modelling system as a tool for air quality management: Annual high-resolution simulations and evaluation, Sci. Total Environ., 390, 323–340, 2008.
Haywood, J. M. and Ramaswamy, V.: Global sensitivity studies of the direct radiative forcing due to anthropogenic sulfate and black carbon aerosols, J. Geophys. Res., 103, 6043–6058, 1998.
Hong, S. Y. and Pan, H. L.: Nonlocal boundary layer vertical diffusion in a Medium-Range Forecast model, Mon. Weather Rev., 124, 2322–2339, 1996.
Hong, S.-Y., Noh, Y., and Dudhia, J.: A new vertical diffusion package with an explicit treatment of entrainment processes, Mon. Weather Rev., 134, 2318–2341, 2006.

Hong, S. Y. and Lim, J. O. J.: The WRF single-moment 6-class microphysics scheme (WSM6), J. Korean. Meteor. Soc., 42, 129–151, 2006.
Hong, S. Y., Noh, Y., and Dudhia, J.: A new vertical diffusion package with an explicit treatment of entrainment processes, Mon. Weather Rev., 134(9), 2318–2341, 2006.
Horowitz, L. W., Walters, S., Mauzerall, D. L., Emmons, L. K., Rasch, P. J., Granier, C., Tie, X., Lamarque, J.-F., Schultz, M. G., Tyndall, G. S., Orlando, J. J., and Brasseur, G. P.: A global simulation of tropospheric ozone and related tracers: description and evaluation of MOZART, Version 2, J. Geophys. Res., 108(D24), 4784, doi:10.1029/2002JD002853, 2003.
Hov, O., Stordal, F., and Eliassen, A.: Photochemical oxidant control strategies in Europe: a 19 days case study using a Lagrangian model with chemistry, vol. TR5/95, NILU, 1985.
Jeuken, A.: Evaluation of chemistry and climate models using measurements and data assimilation, PhD thesis, Eindhoven University of Technology, 2000.
Kasibhatla, P., Chameides, W. L., and John, J. S.: A three-dimensional global model investigation of seasonal variations in the atmospheric burden of anthropogenic sulphate aerosols, J. Geophys. Res., 102, 3737–3759, 1997.
Kaufman, Y. J., Tanré, D., and Boucher, O.: A satellite view of aerosols in the climate system, Nature, 419, 215–223, 2002.
Kesarkar, A. P., Dalvi, M., Kaginalkar, A., and Ojha, A.: Coupling of the Weather Research and Forecasting Model with AERMOD for pollutant dispersion modeling, A case study for PM_{10} dispersion over Pune, India, Atmos. Environ., 41, 1976–1988, 2007.
Kulmala, M., Laaksonen, A., and Pirjola, L.: Parameterization for sulfuric acid/water nucleation rates, J. Geophys. Res., 103(D7), 8301–8307, 1998.
Lattuati, M.: Contribution à l'étude du bilan de l'ozone troposphérique à l'interface de l'Europe et de l'Atlantique Nord: modélisation lagrangienne et mesures en altitude, Thèse de sciences, Université Paris, 6, France, 1997.
Loon van, M., Roemer, M., and Builtjes, P.: Model intercomparison in the framework of the review of the Unified EMEP model, TNO-Report R 2004/282, 2004.
Madronich, S. and Flocke, S.: The Role of Solar Radiation in Atmospheric Chemistry, Handbook of Environmental Chemistry, 1–26, 1998.
Maffeis, G.: Establishment of a yearly gas-PM emission inventory in the great Milan area, TerrAria s.r.l., contract no. 19536-2002-06 FISC ISP IT, Milan, 2002.
Moshammer, H. and Neuberger, M.: The active surface of suspended particles as a predictor of lung function and pulmonary symptoms in Austrian school children, Atmos. Environ., 37,

1737–1744, 2003
Menut, L., Coll, I., and Cautenet, S.: Impact of meteorological data resolution on the forecasted ozone concentrations during the ESCOMPTE IOP 2a and 2b, Atmos. Res., ESCOMPTE Special Issue, 74, 139–159, 2005.
Michelson, S. A. and Bao, J.-W.: Comparison of two meteorological community models for air-quality applications, 14th Joint Conference on the Applications of Air Pollution Meteorology with the Air and Waste Management Association, Am. Meteorol. Soc., J2.7, online available at: ams.confex.com/ams/pdfpapers/102537.pdf, 2006.
Minguzzi, E., Bedogni, M., Carnevale, C., and Pirovano, G.: Sensitivity of CTM simulations to meteorological input, Int. J. Environ. Pollut., 24, 36–50, 2005.
Mlawer, E. J., Taubman, S. J., Brown, P. D., Iacono, M. J., and Clough, S. A.: Radiative transfer for inhomogeneous atmospheres: RRTM, a validated correlated-k model for the longwave, J. Geophys. Res., 102(D14), 16663–16682, 1997.
Moshammer, H. and Neuberger, M.: The active surface of suspended particles as a predictor of lung function and pulmonary symptoms in Austrian school children, Atmos. Environ., 37, 1737–1744, 2003.
Moucheron, M. C. and Milford, J.: Development and Testing of a Process Model for Secondary Organic Aerosols, Air and Waste Management Association, Nashville, TN, USA, 1996.
Nenes, A., Pilinis, C., and Pandis, S. N.: ISORROPIA: a new thermodynamic model for inorganic multicomponent atmospheric aerosols, Aquat. Geochem., 4, 123–152, 1998.
Odum, J. R., Hoffmann, T., Bowman, F., Collins, D., Flagan, R. C., and Seinfeld, J. H.: Gas/particle partitioning and secondary aerosol yield, Environ. Sci. Technol., 30, 2580–2585, 1996.
Odum, J. R., Jungkamp, T. P. W., Griffin, R. J., Flagan, R. C., and Seinfeld, J. H.: The atmospheric aerosol-forming potential of whole gasoline vapour, Science, 276, 96–99, 1997.
Pandis, S. N. and Seinfeld, J. H.: Sensitivity analusis of a chemical mechanism for aqueous-phase atmospheric chemistry, J. Geophys. Res., 94, 1105–1126, 1989.
Pankow, J. F.: An absorption model of gas/particle partitioning of organic compounds in the atmosphere, Atmos. Environ., 28, 185–188, 1994.
Pankow, J. F., Seinfeld, J. H., Asher, W. E., and Erdakos, G. B.: Modeling the formation of secondary organic aerosol, 1. Application of theoretical principles to measurements obtained in the a-pinene/, b-pinene/, sabinene, D3-carene/, and cyclohexene/ozone systems, Environ. Sci. Technol., 35, 1164–1172, 2001.

Penner, J. E., Chuang, C. C., and Grant, K.: Climate forcing by carbonaceous and sulfate aerosols, Clim. Dynam., 14, 839–851, 1998.
Pirovano, G., Coll, I., Bedogni, M., Alessandrini, S., Costa, M. P., Gabusi, V., Lasry, F., Menut, L., and Vautard, R.: On the influence of meteorological input on photochemical modelling of a severe episode over a costal area, Atmos. Environ., 41, 6445–6464, doi:10.1016/j/atmosenv.2007.04.001, 2007.
Schaap, M.: On the importance of aerosol nitrate in Europe, Data analysis and modelling, Ph.D. thesis University of Utrecht, The Netherlands, online available at: http://www.library.uu.nl/digiarchief/dip/diss/2003-1209-110044/inhoud.htm, 2003.
Schaap, M., van Loon, M., ten Brink, H. M., Dentener, F. J., and Builtjes, P. J. H.: Secondary inorganic aerosol simulations for Europe with special attention to nitrate, Atmos. Chem. Phys., 4, 857–874, 2004, http://www.atmos-chem-phys.net/4/857/2004/.
Schaap, M., Denier van der Gon, H. A. C., Visschedijk, A. J. H., Van Loon, M., ten Brink, H. M., Dentener, F. J., Putaud, J.-P., Guillaume, B., Liousse, C., and Builtjes, P. J. H.: Anthropogenic black carbon and fine aerosol distribution over Europe , J. Geophys. Res., 109, D18201, doi:10.1029/2003JD004330, 2004.
Schaap, M., Vautard, R., Bergström, R., van Loon, M., Bessagnet, B., Brandt, J., Christensen, J., Cuvelier, K., Foltescu, V., Graff, A., Jonson, J., Kerschbaumer, A., Krol, M., Langner, J., Roberts, P., Rouil, L., Stern, R., Tarrason, L., Thunis, P., Vignati, E., White, L., Wind, P., and Builtjes, P.: Evaluation of long term aerosol simulations from seven regional air quality models and their ensemble in the EURODELTA study, Atmos. Environ., 41, 2083–2097, 2007.
Schell, B., Ackermann, I. J., Hass, H., Binkowski, F. S., and Ebel, A.: Modeling the formation of secondary organic aerosol within a comprehensive air quality model system, J. Geophys. Res., 106(D22), 28275–28293, 2001.
Schmidt, H., Derognat, C., Vautard, R., and Beekmann, M.: A comparison of simulated and observed ozone mixing ratios for the summer of 1998 in Western Europe, Atmos. Environ., 35(36), 6277–6297, 2001.
Seinfeld, J. H. and Pandis, S. N.: Atmospheric Chemistry and Physics, Wiley, New York, USA, 1998.
Skamarock W. C., Klemp, J. B., Dudhia, J., Gill, D. O., Barker, D. M., Wang, W., and Powers., J. G.: A Description of the Advanced Research WRF Version 2., NCAR Technical Note 468+STR, Mesoscale and Microscale Meteorology Division, NCAR, Boulder, Colorado,

USA, June 2005.
Skamarock, W. C., Klemp, J. B., Dudhia, J., Gill, D. O., Barker, D. M., Wang, W., and Powers, J. G.: A Description of the Advanced Research WRF Version 2, NCAR/TN-468+STR, NCAR Technical Note, Boulder, Colorado, USA, January 2007.
Stern, R., Builtjes, P., Schaap, M., Timmermans, R., Vautard, R., Hodzic, A., Memmesheimer, M., Feldmann, H., Renner, E., Wolke, R., and Kerschbaumer, A.: A model inter-comparison study focussing on episodes with elevated PM_{10} concentrations, Atmos. Environ., 4567–4588, doi:10.1016/j.atmosenv.2008.01.068, 2008.
Stull, R.: An Introduction to Boundary Layer Meteorology, Kluwer Academic Publishers, 1988.
Soong, S.-T., Martien, P. T., Archer, C. L., Tanrikulu, S., Wilczak, J. M., Bao, J.-W., Michelson, S. A., Jia, Y., and Emery, C. A.: Comparison of WRF/CAMx and MM5/CAMx simulations for an ozone episode in California, Eighth Conference on Atmospheric Chemistry, Atlanta, Georgia, USA, 29 January–2 February 2006, 2006.
Thunis, P., Rouil, L., Cuvelier, C., Bessagnet, B., Builtjes, P., Douros, J., Kerschbaumer, A., Pirovano, G., Schaap, M., Stern, R., and Tarrason, L.: Analysis of large and fine scale model responss to emission-reduction scenarios within the CityDelta project, Atmos. Environ., 41(10), 2083–2097, 2007.
Troen, I. and Mahrt, L.: A simple model of the atmospheric boundary layer: Sensitivity to surface evaporation, Bound. Lay. Meteorol., 37, 129–148, 1986.
Tsyro, S.: First estimates of the effect of aerosol dynamics in the calculation of PM_{10} and $PM_{2.5}$, EMEP Report, online available at: http://www.emep.int, 2002.
Vautard, R., Builtjes, P., Thunis, P., Cuvelier, K., Bedogni, M., Bessagnet, B., Honoré, C., Moussiopoulos, N., Schaap, M., Stern, R., Tarrason, L., and van Loon, M.: Evaluation and intercomparison of Ozone and PM_{10} simulations by several chemistry-transport models over 4 European cities within the City-Delta project, Atmos. Environ., 41, 173–188, 2007.
Wesely, M. L.: Parameterization of surface resistances to gaseous dry deposition in regional-scale numerical models, Atmos. Environ., 23, 1293–1304, 1989.
West, J. J., Pilinis, C., Nenes, A., and Pandis, S. N.: Marginal direct climate forcing by atmospheric aerosols, Atmos. Environ., 32, 2531–2542, 1998.
Zhong, S., In, H., and Clements, C.: Impact of turbulence, land surface, and radiation parameterizations on simulated boundary layer properties in a coastal environment, J. Geophys. Res., 112, D13110, doi:10.1029/2006JD008274, 2007.

Table 1. Overview of the chemical and physical processes which are included in the air chemistry transport model CHIMERE. For a more detailed description of the processes in CHIMERE, see Bessagnet et al., 2004.

Process type	Reference
Chemistry	MELCHIOR2, based on Lattuati 1997
Dry deposition	Seinfeld and Pandis, 1998
Photolysis rate constants	Tropospheric Ultraviolet Visible module (TUV), Madronich and Flocke 1998
Wet deposition In cloud and below cloud scavenging of gases and aerosols	Guelle et al., 1998 and Tsyro 2002.
Aerosols	ISORROPIA, Nenes et al., 1998
Coagulation	Fuchs, 1964
Nucleation	Kulmala et al., 1998
Condensation/evaporation	Yes
Cloud effects on photolysis rates	Yes, see Bessagnet et al., 2004
Transport	Parabolic Piecewise Method (PPM), Colella and Woodward (1984)
Vertical diffusion	Troen and Mahrt, 1986
Turbulent transport	Stull, 1988
Cloud chemistry of SO_2 oxidation by H_2O_2 and O_3	Yes
Anthropogenic and Biogenic aerosol formation	Yes, Anthropogenic yields come from Grosjean and Seinfeld (1989), Moucheron and Milford (1996), Odum et al., (1996, 1997) and Schell et al.,(2001). Biogenic aerosol yields for terpene oxidation according to Pankow et al., (1994, 2001)
Vertical structure	8 hybrid sigma pressure levels up to ±5500 m

ACPD
9, 2319–2380, 2009

Table 2. Overview of the WRF and MM5 parameterisations, which are used to create the meteorological input for CHIMERE.

Parameter	WRF	MM5
Integration time step [s]	30	18
Radiation calculation frequency [min]	5	30
Snow cover effects	Yes (Noah)	Yes (Noah)
Cloud effect on radiation	Yes	Yes
Microphysics	WSM6 (mix phase)	4 (simple ice)
Cumulus scheme	None	None
PBL	YSU (MRF successor)	MRF
Radiation	RRTM	RRTM
LSM	Noah	Noah
Surface Layer	Monin-Obukhov	Monin-Obukhov

ACPD
9, 2319–2380, 2009

Table 3a. Statistics for the temperature at the 2 m height.

Time period/ station	Parameter/ model	Relative BIAS [%]		BIAS [°C]		RMSE [°C]			SD [°C]		*R* squared [°C]		NR OBS	MEAN OBS [°C]
		WRF	MM5	WRF	MM5	WRF	MM5	OBS	WRF	MM5	WRF	MM5		
YEAR	ISPRA	2.86	−18.06	0.38	−2.37	3.12	3.87	8.77	7.98	8.41	0.88	0.88	7958	13.12
	ERBA	−11.23	−15.93	−1.20	−1.70	3.62	3.72	8.86	8.10	7.92	0.85	0.86	6929	10.69
	CANTU	4.45	−3.20	0.50	−0.36	3.07	2.88	9.57	8.58	8.57	0.90	0.91	8521	11.15
	SERMIDE	−9.16	−11.11	−1.24	−1.51	2.30	2.45	8.95	9.39	9.10	0.96	0.96	8724	13.57
	MANTOVA	−20.56	−23.54	−3.16	−3.62	3.88	4.27	9.84	9.50	9.05	0.95	0.95	8285	15.37
JANUARY	ISPRA	89.80	−65.74	1.73	−1.27	4.31	4.12	4.90	3.45	3.30	0.36	0.36	742	1.92
	ERBA	31.56	12.33	0.69	0.27	3.03	3.12	4.07	3.71	3.63	0.49	0.44	742	2.18
	CANTU	299.7	159.5	1.79	0.95	4.36	4.21	5.17	3.56	3.19	0.41	0.37	742	0.60
	SERMIDE	−31.31	−54.71	−0.68	−1.19	2.00	2.30	2.64	2.52	2.48	0.54	0.50	742	2.18
	MANTOVA	−58.10	−68.55	−1.79	−2.11	2.55	2.89	2.73	2.72	2.70	0.59	0.52	610	3.09
JUNE	ISPRA	−1.60	−10.21	−0.35	−2.20	3.27	3.82	5.82	3.97	4.75	0.71	0.71	720	21.55
	ERBA	−14.26	−16.26	−3.26	−3.71	3.95	4.23	5.63	4.54	4.44	0.85	0.91	720	22.84
	CANTU	−1.22	−3.99	−0.26	−0.84	2.39	2.17	5.94	4.73	4.87	0.85	0.90	648	21.15
	SERMIDE	−5.92	−6.56	−1.38	−1.53	2.02	2.43	4.98	5.55	5.85	0.94	0.91	696	23.34
	MANTOVA	−15.50	−17.36	−4.04	−4.53	4.40	4.86	5.75	5.51	5.54	0.91	0.91	720	26.09

ACPD
9, 2319–2380, 2009

Table 3b. Statistics for the relative humidity at the 2 m height.

Time period/ station	Parameter/ model	Relative BIAS [%]		BIAS [%]		RMSE [%]			SD [%]		*R* squared [%]		NR OBS	MEAN OBS [%]
		WRF	MM5	WRF	MM5	WRF	MM5	OBS	WRF	MM5	WRF	MM5		
YEAR	ISPRA	−7.32	−3.11	−5.35	−2.27	17.60	19.98	23.96	17.23	17.57	0.51	0.34	7957	73.07
	ERBA	3.58	−2.37	2.30	−1.52	14.64	16.72	20.86	17.05	18.58	0.50	0.41	7001	64.21
	CANTU	4.46	−1.25	3.04	−0.85	16.45	18.97	23.68	18.25	18.81	0.53	0.39	7758	68.26
	SERMIDE	–	–	–	–	–	–	–	–	–	–	–	0	–
	MANTOVA	4.27	5.77	2.86	3.87	12.68	13.49	21.03	19.24	17.91	0.66	0.62	7215	67.09
JANUARY	ISPRA	−12.85	−13.19	−9.72	−9.98	26.48	30.73	28.22	21.05	21.17	0.28	0.11	742	75.65
	ERBA	−8.72	−17.21	−5.72	−11.29	19.02	24.39	22.86	17.15	18.71	0.37	0.22	742	65.62
	CANTU	1.96	−9.29	1.31	−6.23	17.86	22.82	26.38	20.05	21.88	0.54	0.34	407	67.10
	SERMIDE	–	–	–	–	–	–	–	–	–	–	–	0	–
	MANTOVA	−4.00	−9.13	−3.36	−7.66	10.33	15.31	14.50	18.36	18.09	0.61	0.45	198	83.90
JUNE	ISPRA	−8.03	−4.49	−5.71	−3.20	16.91	16.30	22.73	13.36	14.83	0.53	0.51	720	71.18
	ERBA	13.53	9.74	7.73	5.56	13.94	14.28	17.29	14.55	16.59	0.50	0.44	720	57.12
	CANTU	18.90	12.68	10.60	7.11	16.87	15.57	18.83	14.53	16.72	0.52	0.49	720	56.07
	SERMIDE	–	–	–	–	–	–	–	–	–	–	–	0	–
	MANTOVA	12.94	17.13	6.82	9.02	12.04	14.03	16.78	16.06	17.31	0.67	0.64	720	52.68

ACPD
9, 2319–2380, 2009

Table 3c. Statistics for the wind speed.

Time period/ station	Parameter/ model	Relative BIAS [%]		BIAS [m/s]		RMSE [m/s]		SD [m/s]			*R* squared [m/s]		NR OBS	MEAN OBS [m/s]
		WRF	MM5	WRF	MM5	WRF	MM5	OBS	WRF	MM5	WRF	MM5		
YEAR	ISPRA	0.42	−31.01	0.01	−0.78	2.29	1.92	0.75	2.31	1.68	0.04	0.02	8757	2.52
	ERBA	–	–	–	–	–	–	–	–	–	–	–	0	–
	CANTU	–	–	–	–	–	–	–	–	–	–	–	0	–
	SERMIDE	–	–	–	–	–	–	–	–	–	–	–	0	–
	MANTOVA	522.1	473.3	2.20	1.99	2.80	2.56	0.25	1.81	1.70	0.16	0.08	6479	0.42
JANUARY	ISPRA	23.41	−30.58	0.63	−0.82	2.80	1.98	0.66	3.11	2.01	0.43	0.22	742	2.69
	ERBA	–	–	–	–	–	–	–	–	–	–	–	0	–
	CANTU	–	–	–	–	–	–	–	–	–	–	–	0	–
	SERMIDE	–	–	–	–	–	–	–	–	–	–	–	0	–
	MANTOVA	599.4	751.4	2.15	2.69	2.67	3.34	0.24	1.71	1.83	0.02	0.02	127	0.36
JUNE	ISPRA	12.71	−11.56	0.24	−0.22	1.80	1.29	0.55	1.78	1.17	0.02	0.00	720	1.87
	ERBA	–	–	–	–	–	–	–	–	–	–	–	0	–
	CANTU	–	–	–	–	–	–	–	–	–	–	–	0	–
	SERMIDE	–	–	–	–	–	–	–	–	–	–	–	0	–
	MANTOVA	430.7	357.8	2.18	1.81	2.73	2.19	0.24	1.69	1.28	0.08	0.09	719	0.51

Table 3d. Statistics for the wind direction.

Time period/ station	Parameter/ model	Relative BIAS [%]		BIAS [°]		RMSE [°]		SD [°]			*R* squared [°]		NR OBS	MEAN OBS [°]
		WRF	MM5	WRF	MM5	WRF	MM5	OBS	WRF	MM5	WRF	MM5		
YEAR	ISPRA	−39.85	−37.63	−110.9	−104.7	137.7	147.6	19.48	78.69	102.3	0.00	0.00	8757	278.3
	ERBA	–	–	–	–	–	–	–	–	–	–	–	0	–
	CANTU	–	–	–	–	–	–	–	–	–	–	–	0	–
	SERMIDE	–	–	–	–	–	–	–	–	–	–	–	0	–
	MANTOVA	210.7	222.2	112.8	119.0	159.8	166.8	62.24	97.72	103.5	0.00	0.00	6479	53.52
JANUARY	ISPRA	−46.34	−40.29	−130.4	−113.4	148.6	142.2	12.14	65.55	82.8	0.16	0.03	742	281.4
	ERBA	–	–	–	–	–	–	–	–	–	–	–	0	–
	CANTU	–	–	–	–	–	–	–	–	–	–	–	0	–
	SERMIDE	–	–	–	–	–	–	–	–	–	–	–	0	–
	MANTOVA	25.00	38.93	46.18	71.92	127.4	123.8	86.77	98.23	101.7	0.00	0.01	127	184.7
JUNE	ISPRA	−38.07	−40.08	−102.7	−108.2	133.4	153.65	26.41	81.06	105.2	0.00	0.00	720	269.9
	ERBA	–	–	–	–	–	–	–	–	–	–	–	0	–
	CANTU	–	–	–	–	–	–	–	–	–	–	–	0	–
	SERMIDE	–	–	–	–	–	–	–	–	–	–	–	0	–
	MANTOVA	230.3	239.1	106.9	111.0	142.1	148.8	27.67	86.72	95.27	0.01	0.00	719	46.43

ACPD
9, 2319–2380, 2009

Table 3e. Statistics for the time series of rainfall.

Time period/ station	Parameter/ model	Relative BIAS [%]		BIAS [cm]		RMSE [cm]			SD [cm]		*R* squared [cm]		NR OBS	MEAN OBS [cm]
		WRF	MM5	WRF	MM5	WRF	MM5	OBS	WRF	MM5	WRF	MM5		
YEAR	ISPRA	1.75	−19.64	0.0002	−0.0019	0.09	0.07	0.07	0.07	0.04	0.04	0.07	7957	0.0096
	ERBA	8.67	−20.86	0.0010	−0.0024	0.10	0.08	0.08	0.08	0.05	0.05	0.08	8722	0.0114
	CANTU	13.20	−8.53	0.0013	−0.0009	0.10	0.09	0.08	0.08	0.05	0.05	0.05	8415	0.0101
	SERMIDE	23.00	2.96	0.0018	0.0002	0.10	0.08	0.08	0.07	0.04	0.02	0.04	8613	0.0078
	MANTOVA	–	–	–	–	–	–	–	–	–	–	–	0	–
JANUARY	ISPRA	18.24	42.01	0.0001	0.0002	0.01	0.01	0.01	0.01	0.01	0.00	0.00	742	0.0005
	ERBA	9.91	−34.52	0.0001	−0.0004	0.02	0.02	0.02	0.01	0.01	0.00	0.00	742	0.0013
	CANTU	42.52	−3.85	0.0005	0.0000	0.02	0.02	0.02	0.02	0.01	0.00	0.00	742	0.0011
	SERMIDE	482.4	155.4	0.0065	0.0021	0.09	0.02	0.01	0.09	0.02	0.02	0.36	742	0.0013
	MANTOVA	–	–	–	–	–	–	–	–	–	–	–	0	–
JUNE	ISPRA	42.52	2.19	0.0037	0.0002	0.14	0.07	0.07	0.12	0.04	0.00	0.04	720	0.0086
	ERBA	139.8	202.5	0.0094	0.0136	0.09	0.08	0.05	0.10	0.10	0.03	0.41	720	0.0067
	CANTU	38.55	171.2	0.0033	0.0147	0.11	0.12	0.07	0.09	0.12	0.01	0.06	648	0.0086
	SERMIDE	142.0	62.00	0.0027	0.0012	0.07	0.03	0.03	0.06	0.01	0.00	0.00	696	0.0019
	MANTOVA	–	–	–	–	–	–	–	–	–	–	–	0	–

Table 3f. Statistics for the cumulative rainfall.

Time period/ station	Parameter/ model	Relative BIAS [%]		BIAS [cm]		RMSE [cm]			SD [cm]		*R* squared [cm]		NR OBS	MEAN OBS [cm]
		WRF	MM5	WRF	MM5	WRF	MM5	OBS	WRF	MM5	WRF	MM5		
YEAR	ISPRA	−3.71	−22.76	−1.31	−8.02	2.65	9.79	26.58	26.77	21.56	0.99	0.99	7957	35.23
	ERBA	14.44	−12.53	6.12	−5.31	7.25	9.16	33.91	36.65	28.27	0.99	0.98	8722	42.35
	CANTU	29.99	14.65	10.31	5.03	12.50	7.60	28.64	35.33	29.79	0.99	0.96	8415	34.37
	SERMIDE	38.44	21.15	10.21	5.62	12.43	6.12	22.49	27.58	23.81	0.96	0.99	8613	26.57
	MANTOVA	–	–	–	–	–	–	–	–	–	–	–	0	–
JANUARY	ISPRA	97.90	12.45	0.17	0.02	0.20	0.10	0.17	0.08	0.23	0.92	0.82	742	0.17
	ERBA	47.13	−35.42	0.18	−0.14	0.23	0.24	0.47	0.37	0.29	0.94	0.94	742	0.39
	CANTU	89.84	−11.91	0.32	−0.04	0.34	0.10	0.37	0.39	0.36	0.95	0.95	742	0.36
	SERMIDE	701.7	124.2	3.32	0.59	3.48	0.92	0.45	1.49	1.15	0.98	0.98	742	0.47
	MANTOVA	–	–	–	–	–	–	–	–	–	–	–	0	–
JUNE	ISPRA	12.70	−25.80	0.52	−1.07	2.53	1.39	1.92	4.10	2.40	0.83	0.88	720	4.13
	ERBA	164.7	166.4	3.61	3.65	4.91	4.91	1.19	4.40	4.40	0.85	0.90	720	2.19
	CANTU	21.68	91.68	0.61	2.58	1.64	3.64	1.66	2.96	4.07	0.87	0.88	648	2.82
	SERMIDE	146.9	3.81	1.46	0.04	1.61	0.39	0.48	1.14	0.70	0.92	0.73	696	0.99
	MANTOVA	–	–	–	–	–	–	–	–	–	–	–	0	–

ACPD
9, 2319–2380, 2009

Table 4. Monthly mean PM_{10} concentrations calculated by the CHIMERE model using MM5 and WRF meteorology for January 2005, together with the measurements.

Name station	Monthly mean January model with MM5 $\mu g/m^3$	Monthly mean January model with WRF $\mu g/m^3$	Monthly mean January observations $\mu g/m^3$
Ispra	43.2	26.9	57.4
Cantu	43.7	28.7	78.8
Erba	39.5	29.0	67.5
Mantova	64.2	36.7	207
Castelnovo Bariano	51.9	28.6	70.7
Average	48.5	30.0	96.3

Table 5. Monthly mean measured concentrations for Ispra of $SO_4^=$, NO_3^- and NH_4^+ , together with the model calculated mean concentrations using MM5 and WRF, for January 2005.

Mean January 2005, Ispra	EMEP measurement $\mu g/m^3$	CHIMERE MM5 $\mu g/m^3$	CHIMERE WRF $\mu g/m^3$
$SO_4^=$	3.83	1.93	2.57
NO_3^-	9.31	13.4	7.88
NH_4^+	4.21	4.43	3.23
Sum EC,OC, dust	36.3	12.9	8.23

Table 6. Monthly mean PM_{10} concentrations calculated by the CHIMERE model using MM5 and WRF meteorology for June 2005, together with the measurements.

Name station	Monthly mean MM5 June model with $\mu g/m^3$	Monthly mean WRF June model with $\mu g/m^3$	Monthly mean June observations $\mu g/m^3$
Ispra	27.0	25.7	20.1
Cantu	26.9	28.9	31.8
Erba	25.4	30.8	32.7
Mantova	40.6	37.4	39.8
Castelnovo Bariano	29.4	27.4	21.7
Average	29.9	30.0	29.2

Table 7. Monthly mean measured concentrations for Ispra of $SO_4^=$, NO_3^- and NH_4^+ , together with the model calculated mean concentrations using MM5 and WRF, for June 2005.

Mean June 2005, Ispra	EMEP measurement $\mu g/m^3$	CHIMERE MM5 $\mu g/m^3$	CHIMERE WRF $\mu g/m^3$
$SO_4^=$	5.38	5.00	5.65
NO_3^-	1.31	1.73	2.19
NH_4^+	2.33	2.07	2.46
Sum EC,OC, dust	10.53	3.73	4.16

Table 8. Monthly mean ozone values calculated by the CHIMERE model using MM5 and WRF meteorology for June 2005, together with the measurements and the correlation coefficients (based on hourly values).

Name station	Monthly mean model with MM5 (ppb)	Monthly mean model with WRF (ppb)	Monthly mean observations (ppb)	Correlation MM5 vs. Obs	Correlation WRF vs. Obs
Ispra	46.4	52.4	35.3	0.77	0.75
Erba	54.3	56.8	27.6	0.60	0.51
Osio Sotto	42.2	45.8	50.1	0.71	0.57
Gambara	50.1	50.2	49.5	0.47	0.40
Corte de Cortesi	49.5	50.1	41.3	0.75	0.65
Marmirolo Fontana	48.7	49.8	36.6	0.70	0.57
Lecco	52.7	63.5	56.6	0.46	0.63
Varese	41.3	45.9	53.6	0.50	0.35
Chiavenna	49.3	55.8	49.3	0.17	0.45
Milano	31.5	29.5	39.8	0.68	0.41
Average	46.6	50.0	40.0	0.58	0.53

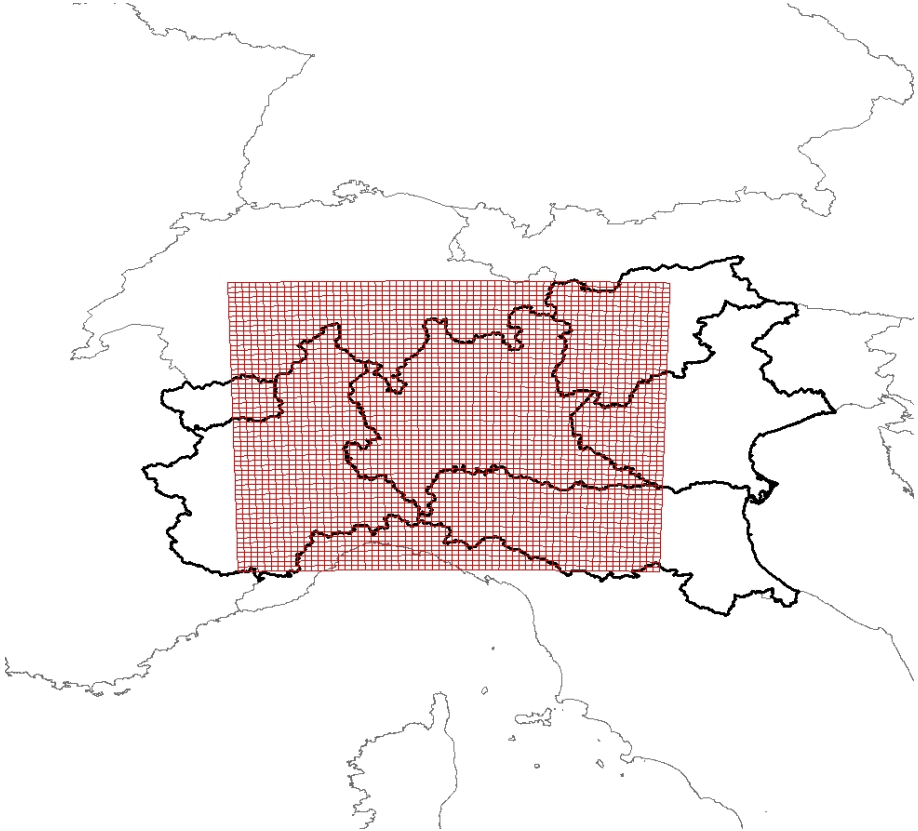

Fig. 1. Map of the location of the model domain in North Italy (centred at 45.0° N, 10.0° E), which covers most of the Po valley, including southern part of the Alps.

ACPD

9, 2319–2380, 2009

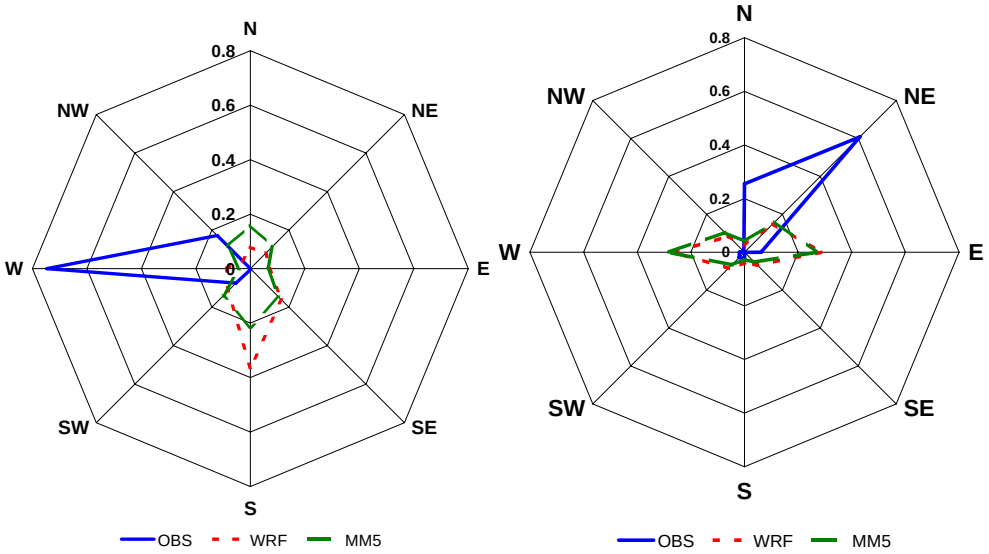

Fig. 2. Wind roses for Ispra (left) and Mantova (right) monitoring stations, annual means. The scale indicates the frequency of the wind direction.

ACPD
9, 2319–2380, 2009

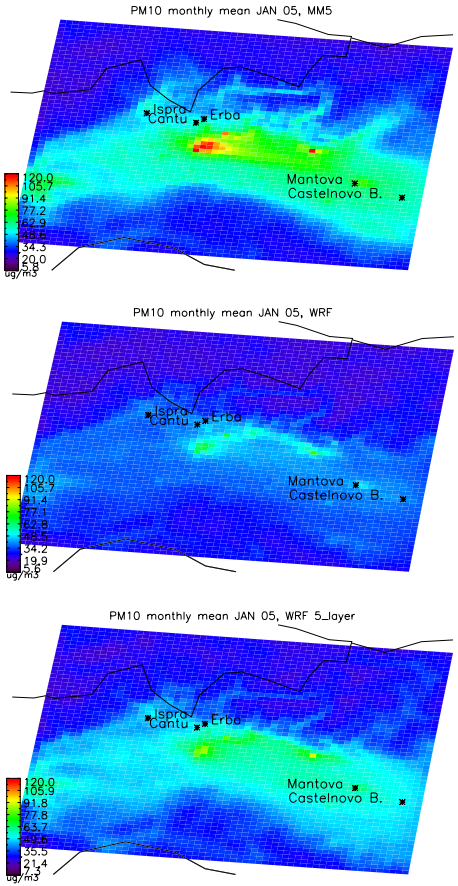

Fig. 3. Monthly mean PM_{10} concentrations for January by CHIMERE using the MM5 meteorology **(a)**, WRF meteorology **(b)** and WRF meteorology using the 5-layer soil temperature model+MRF PBL scheme **(c)**.

ACPD
9, 2319–2380, 2009

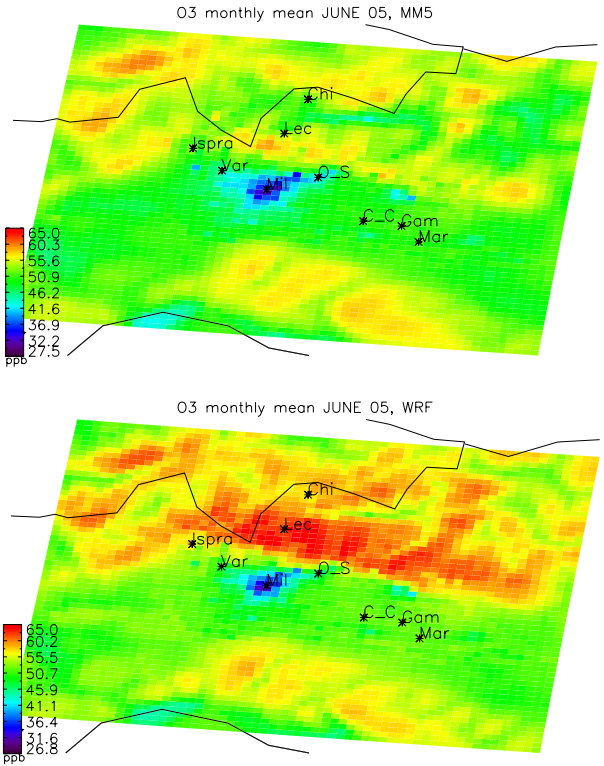

Fig. 4. Monthly mean O_3 concentrations for June by CHIMERE using the MM5 meteorology **(a)** and WRF meteorology, Noah LSM and YSU PBL **(b)**.
Var=Varese, Lec=Lecco, Chi=Chiavenna, O_S=Osio Sotto, C_C=Corte di Cortesi, Gam=Gambara, Mar=Marmirolo Fontana, Mil=Milan.

ACPD
9, 2319–2380, 2009